

# *Phytophthora infestans* RXLR Effector PexRD2 Interacts with Host MAPKKK $\epsilon$ to Suppress Plant Immune Signaling<sup>WJOPEN</sup>

Stuart R.F. King,<sup>a</sup> Hazel McLellan,<sup>b</sup> Petra C. Boevink,<sup>c</sup> Miles R. Armstrong,<sup>b</sup> Tatyana Bukharova,<sup>b</sup> Octavina Sukarta,<sup>b</sup> Joe Win,<sup>d</sup> Sophien Kamoun,<sup>d</sup> Paul R.J. Birch,<sup>b,c</sup> and Mark J. Banfield<sup>a,1</sup>

<sup>a</sup>Department of Biological Chemistry, John Innes Centre, Norwich NR4 7UH, United Kingdom

<sup>b</sup>Division of Plant Sciences, University of Dundee (at James Hutton Institute), Invergowrie, Dundee DD2 5DA, United Kingdom

<sup>c</sup>Cell and Molecular Sciences, James Hutton Institute, Invergowrie, Dundee DD2 5DA, United Kingdom

<sup>d</sup>The Sainsbury Laboratory, Norwich NR4 7UH, United Kingdom

ORCID ID: 0000-0002-6559-3746 (P.R.J.B.)

**Mitogen-activated protein kinase cascades are key players in plant immune signaling pathways, transducing the perception of invading pathogens into effective defense responses. Plant pathogenic oomycetes, such as the Irish potato famine pathogen *Phytophthora infestans*, deliver RXLR effector proteins to plant cells to modulate host immune signaling and promote colonization. Our understanding of the molecular mechanisms by which these effectors act in plant cells is limited. Here, we report that the *P. infestans* RXLR effector PexRD2 interacts with the kinase domain of MAPKKK $\epsilon$ , a positive regulator of cell death associated with plant immunity. Expression of PexRD2 or silencing MAPKKK $\epsilon$  in *Nicotiana benthamiana* enhances susceptibility to *P. infestans*. We show that PexRD2 perturbs signaling pathways triggered by or dependent on MAPKKK $\epsilon$ . By contrast, homologs of PexRD2 from *P. infestans* had reduced or no interaction with MAPKKK $\epsilon$  and did not promote disease susceptibility. Structure-led mutagenesis identified PexRD2 variants that do not interact with MAPKKK $\epsilon$  and fail to support enhanced pathogen growth or perturb MAPKKK $\epsilon$  signaling pathways. Our findings provide evidence that *P. infestans* RXLR effector PexRD2 has evolved to interact with a specific host MAPKKK to perturb plant immunity-related signaling.**

## INTRODUCTION

Plant pathogenic oomycetes and fungi are among the most devastating eukaryotic parasites of socio-economically important food crop species. These filamentous pathogens penetrate plant tissue and extend hyphae into the spaces between cells in search of nutrients. As hyphae extend through plant tissue, they can form intimate contacts with host cells by developing highly specialized structures known as haustoria (Panstruga and Dodds, 2009; Dodds and Rathjen, 2010). These structures are a major interface for exchange of molecules between pathogen and host during infection, including the delivery of pathogen-derived molecules that support infection. These molecules, collectively known as effectors, are thought to be major determinants of pathogenicity, and understanding their molecular functions has become a major theme in the study of plant-microbe interactions. However, our understanding of how filamentous plant pathogen effectors modulate plant immunity is rudimentary.

Plants have developed sophisticated surveillance systems to respond to pathogens and mount defenses against attack (Jones and Dangl, 2006; Dodds and Rathjen, 2010). Defense responses can be initiated at the host cell surface by pattern recognition

receptors (PRRs) that detect evolutionarily conserved molecular signatures of pathogens (pathogen-associated molecular patterns (PAMPs) and PRR-mediated immunity) or apoplastic effector proteins (Boller and Felix, 2009; Win et al., 2012b). In turn, pathogens deliver other effector proteins that function within host cells and interfere with PRR-mediated immunity to promote disease (effector-triggered susceptibility). A second layer of plant immunity monitors for the presence of these foreign translocated effector proteins, directly or indirectly (Chisholm et al., 2006; van der Hooft and Kamoun, 2008; Elmore and Coaker, 2011; Win et al., 2012b). This layer of immunity is intracellular and orchestrated by NB-LRR proteins (plant resistance [R] proteins and NB-LRR-mediated immunity) and can result in localized cell death known as the hypersensitive response (HR). Pathogens also secrete effector proteins that interfere with NB-LRR-mediated immunity. Considerable overlap exists in the downstream signaling cascades activated by PRR- and NB-LRR-mediated immunity, including ion influx, mitogen-activated protein kinase (MAPK) pathways, and increased levels of defense-related hormones. These layers of immunity likely function together as a continuum (Thomma et al., 2011).

In plants, MAPK pathways are important for regulation of development, growth, and the integration of diverse environmental signals, including the response to pathogen attack (Boller and Felix, 2009; Pitzschke et al., 2009; Rodriguez et al., 2010; Meng and Zhang, 2013). MAPK cascades are key players in both PRR- and NB-LRR-mediated immunity (Martin et al., 2003; Boller and Felix, 2009; Segonzac et al., 2011). Phosphorylation of a Thr and a Tyr residue in a Thr-X-Tyr motif, present in the activation loop of MAPKs (Chang and Karin, 2001), regulates diverse plant defense responses, including transcriptional changes. MAPKs are phosphorylated on

<sup>1</sup> Address correspondence to mark.banfield@jic.ac.uk.

The author responsible for distribution of materials integral to the findings presented in this article in accordance with the policy described in the Instructions for Authors (www.plantcell.org) is: Mark J. Banfield (mark.banfield@jic.ac.uk).

<sup>WJOPEN</sup> Online version contains Web-only data.

<sup>OPEN</sup> Articles can be viewed online without a subscription.

www.plantcell.org/cgi/doi/10.1105/tpc.113.120055

these residues by MAPK kinases (MAPKKs); in turn, these MAPKKs are regulated through phosphorylation by MAPKK kinases (MAPKKKs) (Chang and Karin, 2001). A major unanswered question is how perception of diverse stimuli signal through these convergent pathways while maintaining the specificity of the signal. MAPKKKs are often multidomain proteins, and one mechanism of achieving specificity may be through differential protein–protein interactions (Rodriguez et al., 2010). Only a limited number of MAPKKKs have been associated with plant immunity signaling. These include MEKK1 that is activated downstream of the PRR receptor for flagellin in *Arabidopsis thaliana* (Asai et al., 2002; Nicaise et al., 2009); NPK1, a MAPKKK required for triggering an HR response mediated by the N, Bs2, and Rx NB-LRRs (in response to recognition of the p50 protein from tobacco mosaic virus, AvrBs2, and the coat protein of potato virus X, respectively) in *Nicotiana benthamiana* (Jin et al., 2002); MAPKKK $\alpha$ , which is required for the Pto/Prf-mediated response following AvrPto recognition (del Pozo et al., 2004); and EDR1, a negative regulator of defense responses in *Arabidopsis* (Frye et al., 2001). Finally, MAPKKK $\epsilon$  has been identified as important for resistance in tomato (*Solanum lycopersicum*) to certain phytopathogenic bacterial strains and for mediating responses downstream of effector/R protein combinations in *N. benthamiana* (Melech-Bonfil and Sessa, 2010).

Host MAPK signaling pathways are well established as targets of bacterial effector proteins. These effectors have been shown to interfere with signaling from PRR receptors (Göhre et al., 2008; Xiang et al., 2008; Gimenez-Ibanez et al., 2009; Zeng et al., 2012) and coreceptors such as BAK1 (Shan et al., 2008; Cheng et al., 2011). Some of these effectors can covalently modify components of PRR-mediated signaling (Zhang et al., 2010; Feng et al., 2012) and directly inhibit MAPKK and MAPK activity (Zhang et al., 2007, 2012; Wang et al., 2010). However, the extent to which filamentous pathogen effectors target host kinases remains unclear. The *Phytophthora infestans* CRN8 translocated effector is a functional RD kinase (van Damme et al., 2012), but whether this protein interacts with plant kinases is not known. The *Phytophthora sojae* effectors Avh238<sup>P7076</sup> and Avh331 have been shown to interfere with events dependent on MAPK signaling in *Arabidopsis* and *N. benthamiana*, but no association with direct protein–protein interaction was made (Wang et al., 2011; Cheng et al., 2012). Interestingly, no MAPK signaling proteins were identified as effector targets in the plant-pathogen immune network, version 1 (PPIN-1) (Mukhtar et al., 2011).

The hemibiotrophic pathogen *P. infestans* causes late blight, a devastating disease of potato (*Solanum tuberosum*) and tomato (Haas et al., 2009). This pathogen is infamous for devastating European potato crops in the mid-nineteenth century and triggering the Irish potato famine. It still is a critical threat to global food security, causing recurrent epidemics in potato, the third most important food crop (Haas et al., 2009; Cooke et al., 2012; Yoshida et al., 2013). *P. infestans* is a model organism for the study of oomycete pathology (Oliva et al., 2010; Bozkurt et al., 2012) and can infect the model plant *N. benthamiana* (Chaparro-Garcia et al., 2011). To manipulate its hosts, *P. infestans* secretes effector proteins, some of which translocate into host cells (Birch et al., 2006; Kamoun, 2006; Whisson et al., 2007; Schornack et al., 2010). RXLR-type effectors are the largest class of host-translocated proteins in *Phytophthora* (Haas et al., 2009; Raffaele

et al., 2010). The biochemical function of RXLR-type effectors has been localized to their C-terminal domains (Win et al., 2007). Although recent studies have identified the first virulence targets of these proteins in plant cells and provided insight into how they are recognized by NB-LRRs (Bos et al., 2010; Bozkurt et al., 2011; Dong et al., 2011; Saunders et al., 2012), functions for the vast majority of RXLR effectors are not yet known. Despite the diversity in protein sequence displayed within their C-terminal domains, structural studies of RXLR effectors have identified a conserved fold (the WY-domain), predicted to be adopted by many, but not all, of these proteins (Boutemy et al., 2011; Win et al., 2012a).

One *P. infestans* RXLR-type effector that adopts the WY-fold is PexRD2 (Boutemy et al., 2011). PexRD2 is a 121-amino acid protein comprising a signal peptide followed by an RXLR motif (residues 38 to 41, with a degenerate dEER motif spanning residues 48 to 56). The C-terminal effector domain comprises residues 57 to 121. Originally identified in *P. infestans* isolate 88069, PexRD2 is a member of Tribe 6, an 18-member RXLR effector family in *P. infestans* (Haas et al., 2009). Members of this family are predicted, at least in part, to adopt the same WY-domain fold, and some of this family can be modeled on the PexRD2 structure with high confidence scores using IntFOLD (Roche et al., 2011). As such, we predict that this family may have evolved as interaction modules, potentially targeting host proteins of similar structure and function. Typical of most RXLR-type effectors, PexRD2 does not share significant sequence similarity to any protein of known function, making prediction of biochemical activity a challenge. Expression of PexRD2 (lacking the signal peptide) in *N. benthamiana* triggers a weak and delayed dose-dependent cell death response (Oh et al., 2009); a nonspecific cell death response was also recorded on expression in several *Solanum* species (Vleeshouwers et al., 2008). The crystal structure of PexRD2 revealed a homodimeric state with intimate hydrophobic contacts at the interface (Boutemy et al., 2011). Self-association was confirmed in planta, suggesting the dimer is the unit of function.

In this study, we used a yeast two-hybrid (Y2H) screening approach to identify host targets of PexRD2. PexRD2 was shown to interact with MAPKKK $\epsilon$ , a positive regulator of plant immunity-related cell death signaling pathways (Melech-Bonfil and Sessa, 2010). PexRD2 interacts with the kinase domain of MAPKKK $\epsilon$  in yeast and in planta. Overexpression of PexRD2 and virus-induced gene silencing (VIGS) of MAPKKK $\epsilon$  in *N. benthamiana* promoted growth of *P. infestans*. Expression of PexRD2 suppresses both MAPKKK $\epsilon$ -triggered cell death and cell death elicited by combinations of effector/R protein pairs dependent on MAPKKK $\epsilon$ . MAPKKK $\epsilon$ -independent cell death, cell death triggered by MAPKKK $\alpha$ , and cell death triggered by a constitutively active mutant of MAPKK are not affected by expression of PexRD2. Structure-led mutagenesis of PexRD2 revealed the importance of the WY-domain fold and oligomerization of PexRD2 for MAPKKK $\epsilon$  interaction and effector activities. Mutations that disrupt MAPKKK $\epsilon$  interaction result in the loss of all PexRD2 phenotypes. Our results reveal a *P. infestans* RXLR-type effector protein that has evolved to interact with a host MAPKKK to perturb plant immunity-related signaling.

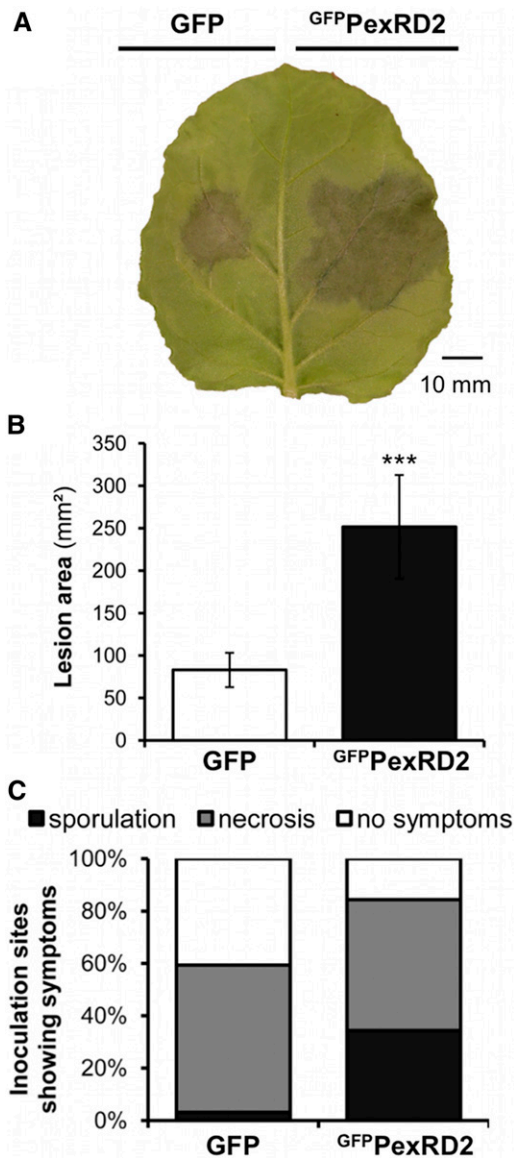


**Figure 1.** Expression of PexRD2 Promotes in Planta Growth and Sporulation of *P. infestans*.

**(A)** Transient expression of GFP PexRD2 in one half of a *N. benthamiana* leaf by agroinfiltration, followed by inoculation with *P. infestans* 88069 zoospores, enhances the growth of the pathogen, compared with expression of GFP in the second half. Image taken at 5 d after zoospore inoculation.

**(B)** Lesion area achieved at 5 d after zoospore inoculation following infection of GFP- or GFP PexRD2-expressing leaf tissue with *P. infestans* 88069. Results are the mean  $\pm$  SE of infections from two independent experiments using at least eight leaves each. The asterisk indicates a value significantly different from the GFP control ( $P < 0.001$ ) as determined by *t* test.

**(C)** Percentage of total inoculation sites showing necrosis and/or sporulation for the same infections.

## RESULTS

### Expression of PexRD2 Promotes in Planta Growth of *P. infestans*

*N. benthamiana* is a host for *P. infestans* and a model for functional studies in the *Solanaceae*. As such, it has been extensively used to investigate host and pathogen gene functions in *P. infestans*–plant interactions (Whisson et al., 2007; Oh et al., 2009; Bos et al., 2010; Bozkurt et al., 2012; Saunders et al., 2012). To investigate whether PexRD2 could benefit *P. infestans* during infection, we used an in planta transient assay (McLellan et al., 2013). In this assay,

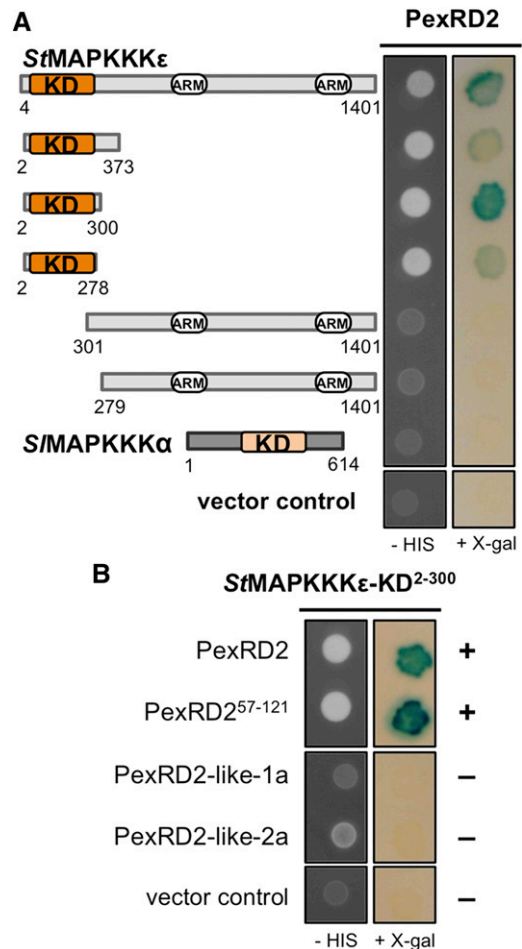


**Figure 2.** PexRD2 Interacts with the Kinase Domain of MAPKKKε.

**(A)** Y2H assay showing that PexRD2 interacts with the kinase domain (KD) of St-MAPKKKε, as evidenced by growth on selective media lacking His (-HIS) and the development of blue coloration in the presence of X-Gal. No interaction was detected between PexRD2 and a second MAPKKK, SI-MAPKKKα.

**(B)** The N-terminal region of PexRD2 (residues 21 to 56, containing the translocation motifs) is not required for the interaction with StMAPKKKε-KD. Furthermore, the two PexRD2-like proteins, PexRD2-like-1a and PexRD2-like-2a, do not interact with StMAPKKKε-KD. The symbols + and - denote interaction and absence of interaction, respectively.

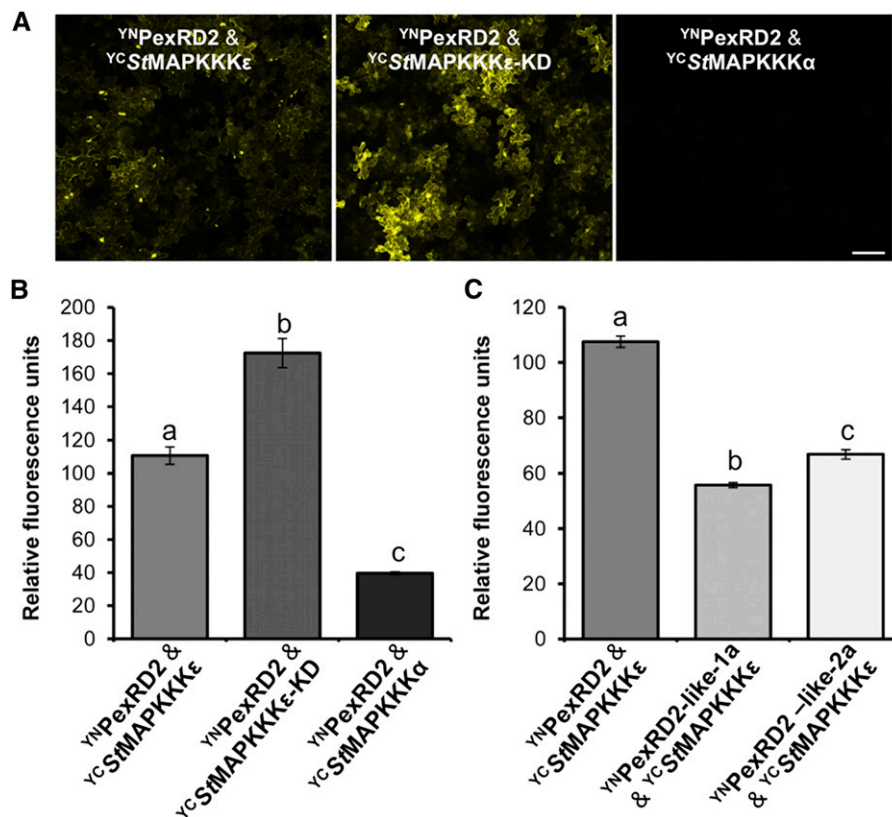


**Figure 3.** PexRD2 and MAPKKK $\epsilon$  Interact in the Plant Cell Cytoplasm.

(A) BiFC of YN PexRD2 with YC StMAPKKK $\epsilon$  (left), YC StMAPKKK $\epsilon$ -KD (middle), and YC StMAPKKK $\alpha$  (right). Bar = 100  $\mu$ m.

(B) Fluorimeter measurements of BiFC shown in (A), each from 36 independent samples.

(C) Fluorimeter measurements of BiFC between YN and YC fusion proteins as indicated, each from 36 independent samples. Results in (B) and (C) are the mean  $\pm$  SE, with the letters indicating values significantly different to each other ( $P < 0.001$ ) as determined by one-way ANOVA.

GFP PexRD2 (GFP PexRD2<sup>21-121</sup>, where a green fluorescent protein tag is substituted for the N-terminal signal peptide) was expressed in one half of *N. benthamiana* leaves via *Agrobacterium tumefaciens*-mediated transient transformation (agroinfiltration) 24 h prior to inoculation with *P. infestans* 88069 zoospores; the second half of the leaves expressed the empty vector control (GFP alone). *P. infestans* 88069 is a standard laboratory strain, particularly appropriate for studying infection of *N. benthamiana* (Chaparro-Garcia et al., 2011). Five days postinoculation, the mean lesion size and mean percentage of inoculation sites sporulating were recorded (Figure 1). The results clearly demonstrate that leaf areas expressing GFP PexRD2 support enhanced *P. infestans* growth compared with the control. This suggests that PexRD2 can act within plant cells to promote effector-triggered susceptibility, supporting *P. infestans* virulence.

#### PexRD2 Interacts with the Kinase Domain of MAPKKK $\epsilon$

To identify putative host targets of PexRD2, we performed a Y2H screen, using a previously described prey library derived from infected potato tissue (Bos et al., 2010), with PexRD2<sup>21-121</sup> (henceforth PexRD2) as bait. The screen involved  $5.9 \times 10^6$

yeast cotransformants. Three transformants were selected from the screen, and each comprised an essentially full-length copy of potato MAPKKK $\epsilon$  (St-MAPKKK $\epsilon$  residues 4 to 1401) (Figure 2A). St-MAPKKK $\epsilon$  is a 154-kD, 1401-amino acid protein with a kinase domain at the N terminus (residues 20 to 274) and two ARM repeat regions (residues 694 to 738 and 1135 to 1220, domains defined by SMART; Letunic et al., 2012). The tomato MAPKKK $\epsilon$  homolog (Sl-MAPKKK $\epsilon$ , 98% amino acid sequence identity to St-MAPKKK $\epsilon$ , 100% in the kinase domain) is a positive regulator of plant immunity signaling pathways (Melech-Bonfil and Sessa, 2010). MAPKKK $\epsilon$  homologs can be identified in a range of dicot plants, including two in *N. benthamiana* (Nb-MAPKKK $\epsilon$ 1 and Nb-MAPKKK $\epsilon$ 2, 90 and 93% identical to St-MAPKKK $\epsilon$ , respectively; 99% identical in the kinase domain) (Melech-Bonfil and Sessa, 2010; Hashimoto et al., 2012). The interaction between PexRD2 and St-MAPKKK $\epsilon$  in yeast was confirmed by retransformation alongside relevant controls.

To map the region of St-MAPKKK $\epsilon$  that interacts with PexRD2, we generated a series of truncations that were tested for interaction with the effector by Y2H. Only the constructs expressing an intact kinase domain enabled growth of yeast on selective plates and the development of blue coloration in the presence of X-Gal (Figure 2A). These results show that the kinase domain of

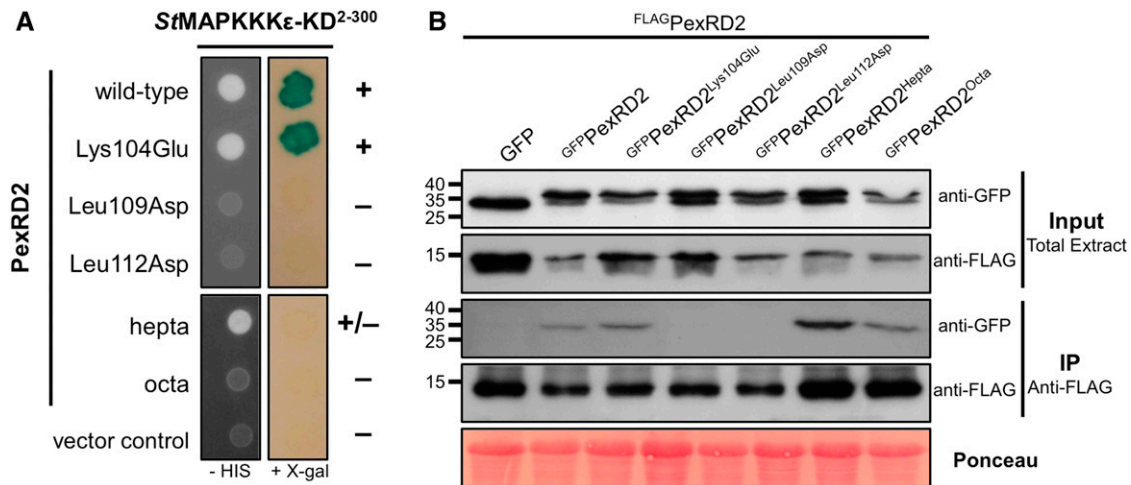


**Figure 4.** Specific Mutants of PexRD2 Show Perturbation in Interaction with MAPKKK $\epsilon$  and in Oligomerization.

**(A)** In Y2H, point mutations in two Leu residues within PexRD2's dimerization interface (Leu109Asp and Leu112Asp), but not the surface presented Lys (Lys104Glu), abolishes the interaction with StMAPKKK $\epsilon$ -KD. Point mutations at nine other individual surface exposed residues also had no effect on the interaction (Supplemental Figure 4). Mutation of seven surface presented residues within a variable region of the WY-domain fold (PexRD2<sup>hepta</sup>) weakens the interaction with StMAPKKK $\epsilon$ -KD. The mutation of an additional surface residue (Ala90Glu) within this region (PexRD2<sup>octa</sup>) leads to a loss of interaction with StMAPKKK $\epsilon$ -KD. The symbols + and - denote interaction and absence of interaction, respectively.

**(B)** In coimmunoprecipitation (IP) from plant tissue, the GFP PexRD2<sup>Leu109Asp</sup> and GFP PexRD2<sup>Leu112Asp</sup> variants do not interact with FLAG PexRD2, suggesting they prevent dimerization. All other GFP-tagged variants tested, that targeted surface-presented residues, retain interaction with FLAG PexRD2.

St-MAPKKK $\epsilon$  (StMAPKKK $\epsilon$ -KD) is both necessary and sufficient for the interaction with PexRD2. As a negative control, we used a second related MAPKKK, SI-MAPKKK $\alpha$  (del Pozo et al., 2004) (which shares 42% sequence identity with St-MAPKKK $\epsilon$  in the kinase domain). No interaction with this kinase was detected (Figure 2A). We also showed that only the WY-domain region of PexRD2 (PexRD2<sup>57-121</sup>) is required for the interaction; the RXLR translocation sequence is dispensable (Figure 2B). This validates the use of the PexRD2 structure (which comprised the effector domain only) as a tool for understanding the interaction between this effector and host proteins.

#### Members of the PexRD2-Like Family Do Not Interact with StMAPKKK $\epsilon$ -KD in Yeast

PexRD2 is a member of a family of 18 RXLR-type effector proteins in *P. infestans* (Haas et al., 2009). To test whether other members of this family might interact with MAPKKK $\epsilon$ , we cloned PexRD2-like-1a and PexRD2-like-2a (PITG\_14984 and PITG\_14787, 47 and 29% sequence identity, respectively, with PexRD2 in the effector domain) into the Y2H bait vector and assayed for interaction with StMAPKKK $\epsilon$ -KD. We found no evidence of interaction (Figure 2B). Immunoblotting confirmed the two PexRD2-like baits were expressed and stable (Supplemental Figure 1).

#### PexRD2 and St-MAPKKK $\epsilon$ Localize to, and Interact, in the Plant Cell Cytoplasm

Confocal microscopy with fluorescent-labeled proteins showed PexRD2 localizes to the plant cell cytoplasm when expressed on its own, together with St-MAPKKK $\epsilon$ , or in the presence of *P. infestans*

infection (Supplemental Methods and Supplemental Figure 2). St-MAPKKK $\epsilon$  is also located to the plant cell cytoplasm.

We used a bimolecular fluorescence complementation (BiFC) approach to examine whether interaction between PexRD2 and St-MAPKKK $\epsilon$  occurs in the cytoplasm. An N-terminal fragment of YFP (YN) was fused to PexRD2 (<sup>YN</sup>PexRD2) and coexpressed, in turn, with a C-terminal fragment of YFP (YC) fused to St-MAPKKK $\epsilon$ , StMAPKKK $\epsilon$ -KD, or SI-MAPKKK $\alpha$ . Cytoplasmic fluorescence, indicative of YFP reconstitution, was observed with <sup>YC</sup>StMAPKKK $\epsilon$  and <sup>YC</sup>StMAPKKK $\epsilon$ -KD, but not with <sup>YC</sup>SI-MAPKKK $\alpha$  (Figures 3A and 3B). Levels of fluorescence were quantified in leaf disks and compared. Significantly increased fluorescence (one way ANOVA) was observed when coexpressing <sup>YC</sup>StMAPKKK $\epsilon$  or <sup>YC</sup>StMAPKKK $\epsilon$ -KD with <sup>YN</sup>PexRD2, when compared with <sup>YC</sup>SI-MAPKKK $\alpha$  (the negative control; Figure 3B).

As these results mirrored interactions observed using Y2H, we extended the analysis to PexRD2-like proteins. Consistent with the Y2H results, significantly less fluorescence (one way ANOVA) was detected following coexpression of <sup>YC</sup>StMAPKKK $\epsilon$  with <sup>YN</sup>-PexRD2-like-1a or <sup>YN</sup>PexRD2-like-2a (Figure 3C). Immunoblots of each construct used for BiFC show that fusion proteins are stable in planta (Supplemental Figure 3).

#### Variants of PexRD2 Perturb Interactions with StMAPKKK $\epsilon$ -KD in Yeast and Disrupt Effector Oligomerization in Planta

Following the in planta confirmation of interaction between PexRD2 and St-MAPKKK $\epsilon$ , we exploited the structure of PexRD2 to design point mutations that might disrupt this interaction (Supplemental Figure 4A) and tested these using the Y2H assay. Two mutations, Leu109Asp and Leu112Asp, were designed to introduce charged

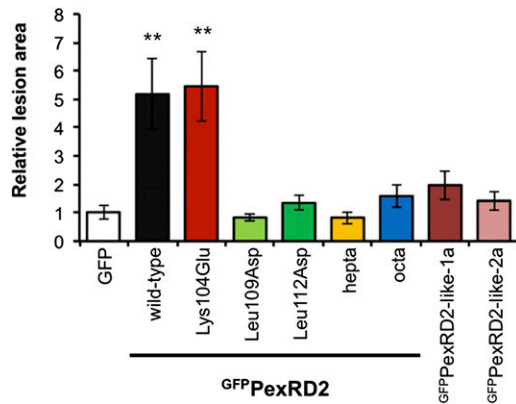


**Figure 5.** PexRD2 Variants Showing Perturbed Interactions with MAPKKK $\epsilon$ , or PexRD2-Like Effectors, Fail to Enhance Pathogen Growth.

Transient expression of wild-type GFP-PexRD2 in one half of a *N. benthamiana* leaf by agroinfiltration, followed by inoculation with *P. infestans* 88069 zoospores, enhances the lesion area achieved at 5 d after zoospore inoculation, relative to the GFP control. A similar level of enhancement was observed for PexRD2<sup>Lys104Glu</sup>. No significant enhancement of pathogen growth was observed for the four variants of PexRD2 that show perturbed interactions with MAPKKK $\epsilon$  (Leu109Asp, Leu112Asp, PexRD2<sup>hepta</sup>, or PexRD2<sup>octa</sup>) or the two PexRD2-like effectors. Results are the mean  $\pm$  SE of infections from two independent experiments using at least eight leaves each time. The asterisks indicate values significantly different from the GFP control ( $P < 0.01$ ) as determined by one-way ANOVA; all other values were not significantly different ( $P > 0.05$ ).

residues into the hydrophobic dimerization interface of PexRD2. An additional 10 mutations, Glu61Ala, Asp74Ala, Asp75Ala, Lys79-Glu, Lys81Glu, Lys85Glu, Glu97Gln, Glu101Gln, Lys104Glu, and Lys107Glu, were introduced to charged surface residues and were designed to minimize any impact on the WY-domain fold. Only Leu109Asp and Leu112Asp prevented the interaction with StMAPKKK $\epsilon$ -KD in yeast (Figure 4A; Supplemental Figure 4B). Immunoblots confirmed the expression of intact fusion proteins for both noninteracting mutants in yeast (Supplemental Figure 4C). Using coimmunoprecipitation from plant tissue, we confirmed that, as expected, the Leu109Asp and Leu112Asp mutations perturb PexRD2 oligomerization in planta (Figure 4B).

We then used the sequence variation between PexRD2 and PexRD2-like-1a, and the structure of PexRD2, to generate mutants within a region of the WY-fold previously shown to accommodate different structures (Boutemy et al., 2011). One of these variants comprised mutations in seven surface-presented residues (Supplemental Figures 5A and 5B). This mutant, PexRD2<sup>hepta</sup>, still supported very weak yeast growth on selective media but did not promote development of blue coloration in the presence of X-Gal (Figure 4A). A second mutant, PexRD2<sup>octa</sup>, that comprised the PexRD2<sup>hepta</sup> background with an additional surface-presented mutation (Ala90Glu), did not interact in the Y2H assays (Figure 4A). These constructs expressed stably in yeast (Supplemental Figure 5C). PexRD2<sup>hepta</sup> and PexRD2<sup>octa</sup> were still able to interact with wild-type PexRD2 in planta, as observed by coimmunoprecipitation (Figure 4B), suggesting these variants retain the ability to oligomerize.

### Noninteracting Mutants of PexRD2 Fail to Enhance Pathogen Growth

To link the observed interaction of PexRD2 and MAPKKK $\epsilon$  with any putative virulence activity, we tested whether PexRD2-like-1a, PexRD2-like-2a, or any of the PexRD2 variants that did not interact with StMAPKKK $\epsilon$ -KD, enhanced the growth of

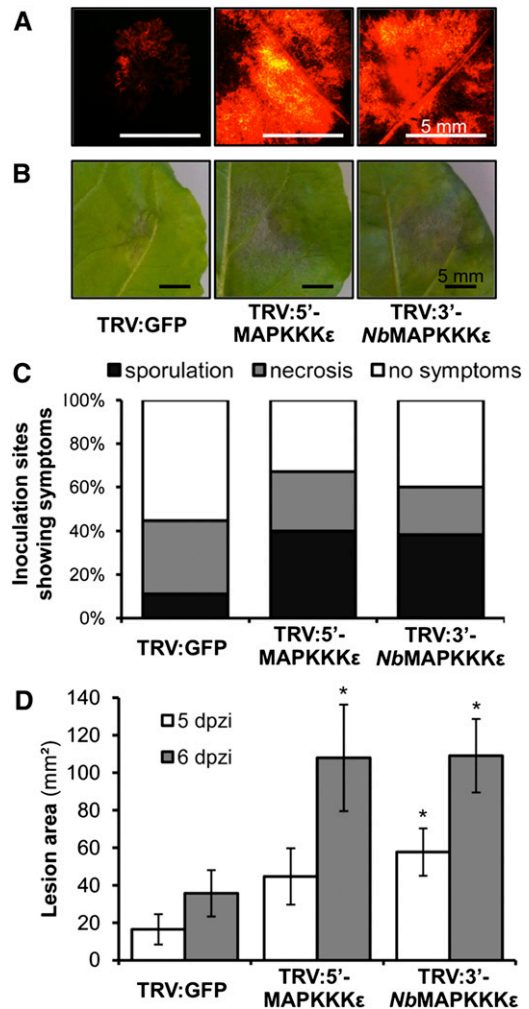


**Figure 6.** VIGS of Nb-MAPKKK $\epsilon$  Enhances Pathogen Growth.

Silencing of MAPKKK $\epsilon$  in *N. benthamiana*, with either TRV:5'-MAPKKK $\epsilon$  or TRV:3'-NbMAPKKK $\epsilon$ , followed by inoculation with zoospores of the red fluorescent *P. infestans* 88069<sup>rd</sup> enhances the growth of the pathogen compared with control silencing with TRV:GFP.

(A) Fluorescence microscopy images taken at 4 d after zoospore inoculation indicate more hyphal growth on the MAPKKK $\epsilon$ -silenced plants. (B) and (C) Silencing MAPKKK $\epsilon$  also enhances the levels of necrosis and sporulation at 5 d after zoospore inoculation.

(D) Lesion area achieved at 5 and 6 d after zoospore inoculation following infection of TRV-treated plants with *P. infestans* 88069<sup>rd</sup>. Results are the mean  $\pm$  SE of 40 inoculations from two independent experiments. Asterisks indicate values significantly different from the TRV:GFP control at the same time point ( $P < 0.05$ ) as determined by one-way ANOVA; all other values were not significantly different ( $P > 0.05$ ).

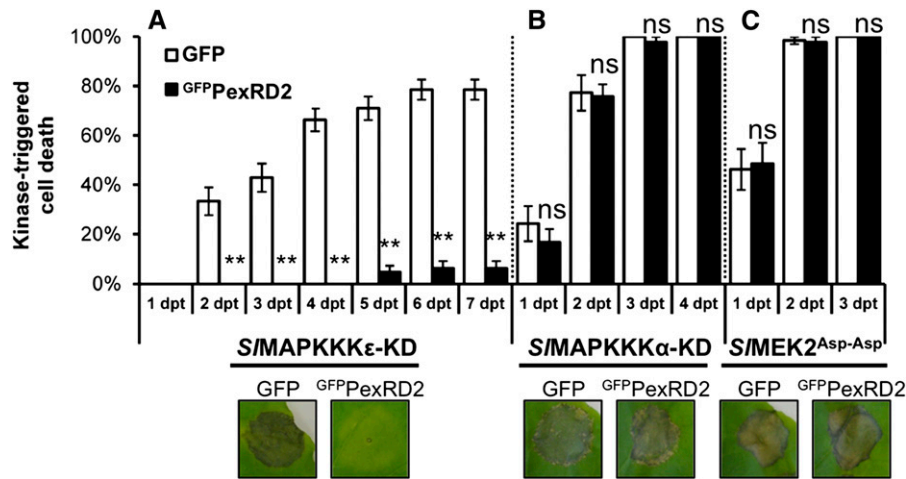


**Figure 7.** MAPKKK $\epsilon$ -Triggered Cell Death Is Suppressed by PexRD2.

Coexpression of GFP:PexRD2 with S/MAPKKK $\epsilon$ -KD in *N. benthamiana* reduces the percentage of infiltration sites with >50% confluent cell death at 2 to 7 d post- $\beta$ -estradiol treatment (dpt) compared with coexpression with the GFP control (A). By contrast, PexRD2 did not suppress the cell death triggered by either the kinase domain of S/MAPKKK $\alpha$ -KD (B) or a constitutively active mutant of the proposed downstream MAPKK, S/MEK2<sup>Asp-Asp</sup> (C). Results are the mean  $\pm$  SE of three independent experiments, each using at least three plants. Asterisks indicate values significantly different from the GFP control at the same time point ( $P < 0.01$ ) as determined by one-way ANOVA; all other values were not significantly different (ns;  $P > 0.05$ ). Images indicate representative infiltration sites at 7 dpt.

*P. infestans* 88069 on *N. benthamiana*. PexRD2<sup>Lys104Glu</sup>, which still interacts with StMAPKKK $\epsilon$ -KD, was included as a positive control. All of the noninteracting variants failed to significantly enhance pathogen growth, as measured by the total lesion area relative to the GFP control on the same leaf (Figure 5). By contrast, GFP:PexRD2<sup>Lys104Glu</sup> enhanced pathogen growth to the same level as the wild type. This implicates the interaction between PexRD2 and MAPKKK $\epsilon$  as critical to this effector's virulence activity. All fusion proteins are expressed in planta (Supplemental Figure 6).

#### Silencing of Nb-MAPKKK $\epsilon$ Enhances Pathogen Growth

Having shown that expression of PexRD2 in *N. benthamiana* enhances pathogen growth, and this effector interacts with MAPKKK $\epsilon$  homologs, we used VIGS of Nb-MAPKKK $\epsilon$  to determine whether the product of this gene has a role in restricting growth of *P. infestans* during infection. We used two VIGS constructs, TRV:5'-MAPKKK $\epsilon$  (Melech-Bonfil and Sessa, 2010) and TRV:3'-NbMAPKKK $\epsilon$  (a construct based on TRV:3'-MAPKKK $\epsilon$ ; Melech-Bonfil and Sessa, 2010), alongside a TRV:GFP control. We observed an  $\sim 70\%$  reduction in endogenous transcripts of Nb-MAPKKK $\epsilon$  in VIGS plants and confirmed that levels of Nb-MAPKKK $\alpha$  were not significantly altered (Supplemental Figure 7). To further assess the potential for off-target silencing, we examined the draft genome of *N. benthamiana* (see Supplemental Methods for further details) (Bombarely et al., 2012). As observed by Melech-Bonfil and Sessa (2010), Nb-MAPKKK $\epsilon$  silencing resulted in a moderate retardation of plant growth.

Leaves detached from plants 14 d postinoculation with TRV constructs were inoculated with *P. infestans* 88069<sup>td</sup> (*P. infestans* 88069 expressing a tandem-dimer red fluorescent protein allowing

visualization of hyphal growth). Plants silenced with either TRV:5'-MAPKKK $\epsilon$  or TRV:3'-NbMAPKKK $\epsilon$  repeatedly showed enhanced growth of pathogen hyphae, visible 3 to 4 d postinoculation (Figure 6A). Furthermore, the growth of necrotic lesions (Figure 6B) and progression to sporulation were accelerated in these plants compared with the TRV:GFP control (Figures 6C and 6D). These results indicate that Nb-MAPKKK $\epsilon$  is likely involved in a plant immune response to *P. infestans* 88069 that can limit infection by the pathogen.

#### MAPKKK $\epsilon$ -Triggered Cell Death Is Suppressed by PexRD2

Expression of either full-length SI-MAPKKK $\epsilon$  or S/MAPKKK $\epsilon$ -KD<sup>1-332</sup> triggers pathogen-independent cell death in *N. benthamiana* and requires an active kinase domain [the P-loop mutant S/MAPKKK $\epsilon$ -KD<sup>1-332(Lys49Arg)</sup> prevents activity; Melech-Bonfil and Sessa, 2010]. To test whether StMAPKKK $\epsilon$ -KD<sup>1-332</sup> and StMAPKKK $\epsilon$ -KD<sup>1-300</sup> also trigger cell death on expression, we cloned these domains into the estradiol-inducible pER8 vector (Zuo et al., 2000) and delivered these into plant cells by agroinfiltration. Two days postagroinfiltration, expression was induced with  $\beta$ -estradiol. All wild-type kinase domains triggered cell death. No cell death was observed following expression of S/MAPKKK $\epsilon$ -KD<sup>Lys49Arg</sup> (Supplemental Figure 8).

We tested the effect of coexpressing GFP:PexRD2 on the cell death triggered by S/MAPKKK $\epsilon$ -KD<sup>1-332</sup>. Two days after coagroinfiltration, expression of SI-MAPKKK $\epsilon$  was induced with  $\beta$ -estradiol. Cell death was then scored for 7 d after  $\beta$ -estradiol treatment (Figure 7A). These assays reveal that PexRD2 is a potent suppressor of the cell death triggered by S/MAPKKK $\epsilon$ -KD. The protein levels of S/MAPKKK $\epsilon$ -KD in the presence or absence of GFP:PexRD2 were confirmed to be similar by immunoblot, indicating that this inhibition is not achieved through any effect on

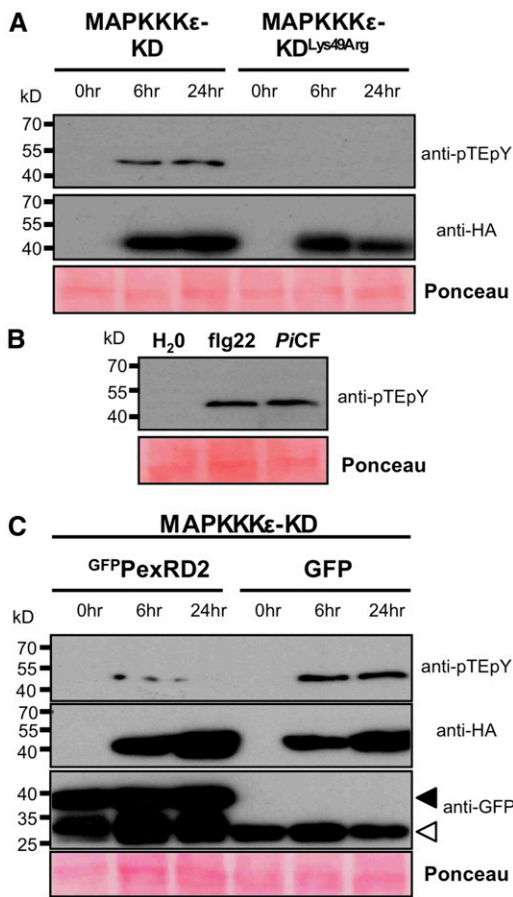


**Figure 8.** MAPKκ-Mediated Activation of MAPKs Is Suppressed by PexRD2.

**(A)** Immunoblot analysis shows that overexpression of *S*MAPKκ-KD causes activation of an endogenous MAPK in *N. benthamiana*. Overexpression of the kinase-inactive mutant (MAPKκ-KD<sup>Lys49Arg</sup>) did not phosphorylate MAPK. Protein levels of both kinases at 6 and 24 h post-β-estradiol treatment were confirmed using an anti-HA antibody (also in **[C]**).

**(B)** Treatment of *N. benthamiana* leaf disks with peptide corresponding to the epitope of the bacterial PAMP flagellin, flg22 (100 nM), or 100-fold diluted *P. infestans* 88069 culture filtrate (PiCF) results in activation of MAPK.

**(C)** Coexpression of GFP<sup>PexRD2</sup>, but not GFP, suppresses the activation of MAPK mediated by *S*MAPKκ-KD. Expression of GFP<sup>PexRD2</sup> and *S*MAPKκ-KD was confirmed using anti-GFP and anti-HA antibodies, respectively. Black arrow indicates expected size of the GFP<sup>PexRD2</sup> fusion protein and the white arrow free GFP. Similar results were observed in three independent experiments. In all cases, protein loading is confirmed by Ponceau staining.

protein expression or stability (Figure 8C). GFP<sup>PexRD2</sup> also suppressed cell death when coexpressed with *St*MAPKκ-KD<sup>1-332</sup> and *St*MAPKκ-KD<sup>1-300</sup> (Supplemental Figure 8). We also tested the effect of GFP<sup>PexRD2</sup> on the cell death triggered by *S*MAPKκ-KD (del Pozo et al., 2004) and a constitutively active variant of the proposed downstream MAPK, *SI*-MEK2 (Melech-Bonfil and Sessa, 2010) or *S*MEK2<sup>Asp-Asp</sup> (Oh and Martin, 2011). No significant difference was observed in the mean level of cell

death observed in GFP<sup>PexRD2</sup> coagroinfiltrated sites compared with GFP control for either *S*MAPKκ-KD (Figure 7B) or *S*MEK2<sup>Asp-Asp</sup> (Figure 7C). These results show that PexRD2 specifically suppresses the macroscopic cell death triggered by MAPKκ kinase domains.

### MAPKκ Promotes Phosphorylation of MAPKs and PexRD2 Suppresses This Activity

We investigated whether overexpression of MAPKκ in plant cells leads to phosphorylation of downstream MAPKs, prior to development of macroscopic cell death, and whether PexRD2 could suppress this. First, we expressed *S*MAPKκ-KD, or the inactive *S*MAPKκ-KD<sup>Lys49Arg</sup>, in *N. benthamiana*, prepared leaf tissue at 6 and 24 h after treatment with β-estradiol and looked for the presence of activated MAPKs using an antibody specific to the phosphorylated Thr-X-Tyr motif of these proteins. We observed a single band in the samples expressing *S*MAPKκ-KD that was absent on expression of *S*MAPKκ-KD<sup>Lys49Arg</sup> (Figure 8A). Following elicitation with flg22, *N. benthamiana* leaf extracts can show single and multiple phosphorylated MAPKs (Segonzac et al., 2011). In our controls, we observed a single band following treatment with flg22 or *P. infestans* culture filtrate (Figure 8B). Coagroinfiltration of GFP<sup>PexRD2</sup> led to a clear reduction in the accumulation of this phosphorylated MAPK band compared with the GFP control (Figure 8C).

### MAPKκ-Dependent Cell Death Is Suppressed by PexRD2

VIGS of MAPKκ in *N. benthamiana* reduces the cell death activated by coexpression of specific fungal and bacterial effectors with their cognate R proteins (Melech-Bonfil and Sessa, 2010). We confirmed these results for the Avr4/Cf4 (*Cladosporium fulvum* effector) and AvrPto/Pto (*Pseudomonas syringae* effector) pairs (Supplemental Figures 9A and 9B). We also tested

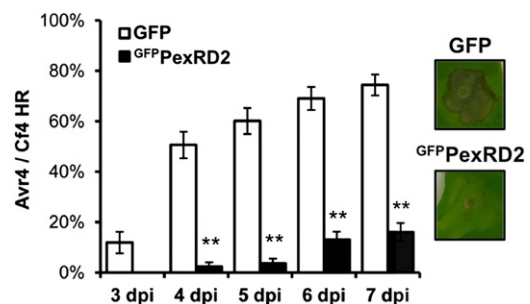


**Figure 9.** PexRD2 Suppresses the Cell Death Associated with the Avr4/Cf4 HR.

Coexpression of GFP<sup>PexRD2</sup> with the both the *C. fulvum* effector Avr4 and tomato resistance protein Cf4 in *N. benthamiana* reduces the percentage of infiltration sites with >50% confluent cell death at 3 to 7 d postagroinfiltration (dpi) compared with the GFP control. Results are the mean ± SE of three independent experiments, each using at least four plants. Asterisks indicate a value significantly different from the GFP control at the same time point ( $P < 0.01$ ) as determined by one-way ANOVA; all other values were not significantly different ( $P > 0.05$ ). Images indicate representative infiltration sites at 7 dpi.

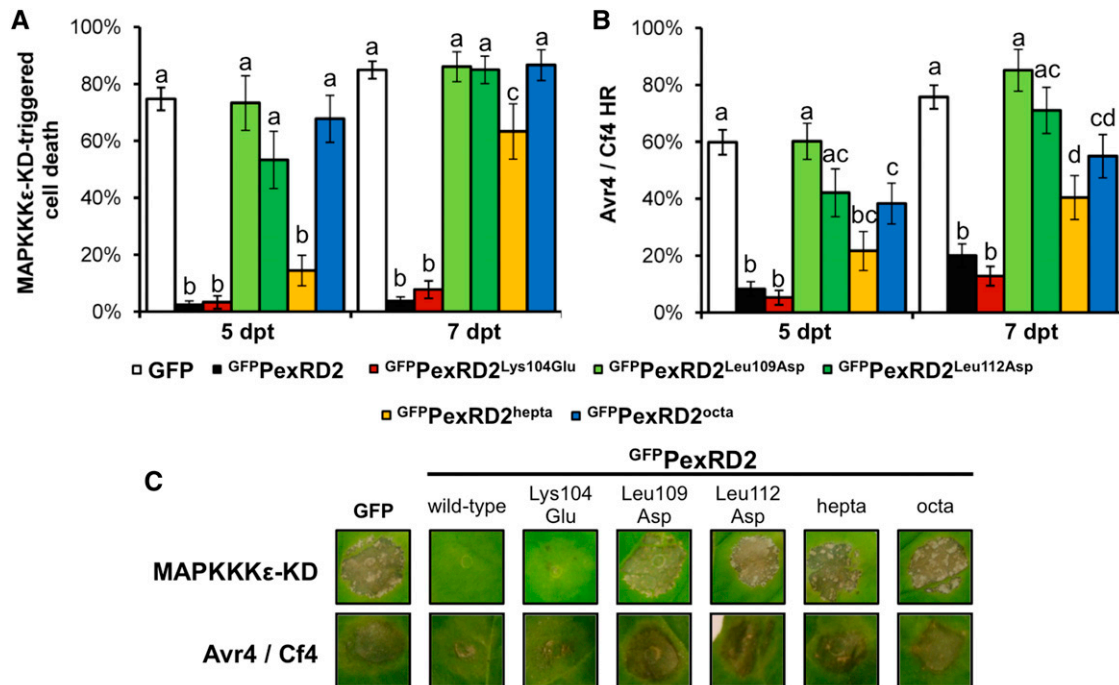


**Figure 10.** PexRD2 Variants That Are Perturbed in MAPKKK $\epsilon$  Interaction Also Show Reduced Suppression of MAPKKK $\epsilon$ -Triggered or MAPKKK $\epsilon$ -Mediated Cell Death.

**(A)** Percentage of infiltration sites with >50% confluent cell death at 5 and 7 d post- $\beta$ -estradiol treatment (dpt), following coexpression of the respective PexRD2 mutants with S/MAPKKK $\epsilon$ -KD.

**(B)** Percentage of infiltration sites with >50% confluent cell death at 5 and 7 d after agroinfiltration (dpi), following coexpression of the respective PexRD2 mutants with Avr4 and Cf4. Results are the mean  $\pm$  SE of three independent experiments, each using at least four plants. The same letter above two bars indicates values that are not significantly different from one another at the same time point ( $P > 0.05$ ) as determined by one-way ANOVA.

**(C)** Images indicate representative infiltration sites at 7 dpt (MAPKKK $\epsilon$ -KD) and 7 dpi (Avr4/Cf4).

whether silencing of Nb-MAPKKK $\epsilon$  reduced cell death in response to the *P. infestans* effector/R protein pair AVR3a<sup>K1</sup>/R3a (Armstrong et al., 2005) or expression of the *P. infestans* effector CRN8 (van Damme et al., 2012) or *P. infestans* elicitor INF1 (Kamoun et al., 1998). No effect on the mean percentage of cell death mediated by these elicitors was observed (Supplemental Figures 9C to 9E), indicating that they are independent of the MAPKKK $\epsilon$  signaling cascade.

We investigated whether PexRD2 interferes with MAPKKK $\epsilon$ -dependent and MAPKKK $\epsilon$ -independent cell death. When coexpressed with either Avr4/Cf4 (Figure 9) or AvrPto/Pto (Supplemental Figure 10A), PexRD2 strongly suppressed macroscopic MAPKKK $\epsilon$ -dependent cell death compared with the GFP control. By contrast, coagroinfiltration of PexRD2 with AVR3aK1/R3a, INF1, or CRN8 did not affect the cell death induced by any of these elicitors (Supplemental Figures 10B to 10D). These experiments reveal a direct correlation in cell death suppressed by either silencing of Nb-MAPKKK $\epsilon$  or coexpression of PexRD2 with the elicitors.

#### PexRD2 Variants That Do Not Interact with MAPKKK $\epsilon$ Do Not Suppress MAPKKK $\epsilon$ -Dependent Cell Death

We tested whether variants of PexRD2 that no longer interact with StMAPKKK $\epsilon$ -KD have lost their ability to suppress MAPKKK $\epsilon$ -

triggered or MAPKKK $\epsilon$ -dependent cell death. We used the noninteracting mutants PexRD2<sup>Leu109Asp</sup>, PexRD2<sup>Leu112Asp</sup>, and PexRD2<sup>octa</sup>, the weakly interacting mutant PexRD2<sup>hepta</sup>, and one interacting mutant PexRD2<sup>Lys104Glu</sup> (as a control) alongside the wild-type protein in coagroinfiltration assays with either S/MAPKKK $\epsilon$ -KD or Avr4/Cf4. All the mutants that failed to interact with StMAPKKK $\epsilon$ -KD in the Y2H assay failed to suppress both MAPKKK $\epsilon$ -triggered and MAPKKK $\epsilon$ -dependent cell death activities (Figure 10). Interestingly, the PexRD2<sup>hepta</sup> mutant showed an intermediate phenotype as it was able to delay, but not prevent, cell death development. This observation corresponds to the strength of interaction between this mutant and StMAPKKK $\epsilon$ -KD in the Y2H (Figure 4). However, this mutant did not demonstrate an enhanced infection phenotype (Figure 5).

#### DISCUSSION

MAPK cascades are well established as key signaling systems in plants, transducing perception of abiotic and biotic stresses to downstream targets, in addition to playing roles in growth and development. In the defense against pathogens, plant MAPK cascades orchestrate changes in defense-related gene expression and other antimicrobial responses (Pitzschke et al., 2009; Meng and Zhang, 2013). Highlighting their importance,

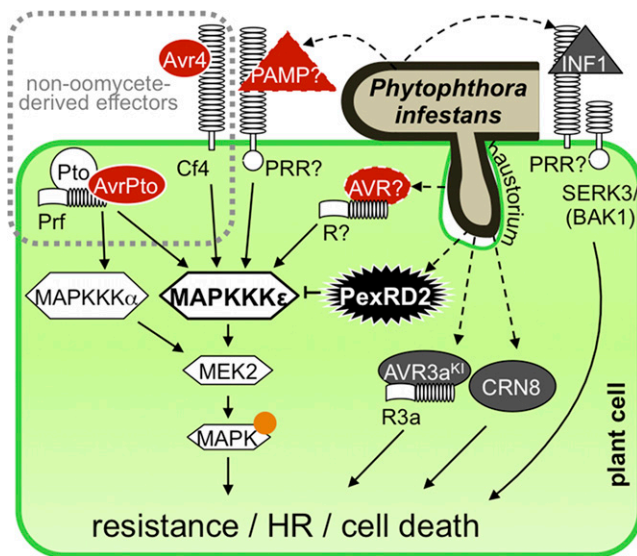


**Figure 11.** Model of PexRD2 Function during Infection.

Schematic diagram illustrating *P. infestans* delivering PexRD2 into a haustoriated plant cell. PexRD2 interacts with MAPKKK $\epsilon$  in the plant cytosol and inhibits signaling by this protein. The cell death triggered by overexpression of MAPKKK $\epsilon$  is inhibited by the presence of PexRD2, but not the cell death triggered by MAPKKK $\alpha$  or MEK2. PexRD2 also suppresses the phosphorylation of MAPKs (orange circle), which occurs following overexpression of MAPKKK $\epsilon$ . The HR following recognition of the *C. fulvum* effector Avr4 by Cf4 and the *P. syringe* effector AvrPto mediated by Pto/Prf, which are known to be MAPKKK $\epsilon$  dependent (red, solid white border), are suppressed by the presence of PexRD2. The HR resulting from the recognition of AVR3a<sup>KI</sup> by R3a, the cell death following recognition of the PAMP-like INF1, and the cell death mediated by CRN8 are all MAPKKK $\epsilon$  independent (dark gray) and are not suppressed by PexRD2. We propose that, in planta, MAPKKK $\epsilon$  confers enhanced resistance against *P. infestans* following recognition of an unidentified PAMP (red triangle, dashed outline), by a PRR or recognized effector/avrulence protein (AVR, red oval, dashed outline) by an R protein. The pathogen delivers PexRD2 inside the host cell to specifically inhibit this MAPKKK $\epsilon$ -dependent resistance and promote proliferation.

bacterial pathogens of plants have evolved translocated effector proteins that interfere with MAPK signaling pathways (Pitzschke et al., 2009; Meng and Zhang, 2013). In this study, we directly link a filamentous plant pathogen effector with components of MAPK signaling in plants. We identify an RXLR-type effector from the late blight pathogen *P. infestans* that interacts with MAPKKK $\epsilon$  and perturbs plant defense-related processes either triggered by or dependent on the activity of this kinase. This establishes MAPK cascades as direct targets of oomycete RXLR-type effectors.

PexRD2 is one of a limited number of RXLR-type effectors for which structural information is available. Here, we used structure-informed mutagenesis of both surface- and dimerization interface-presented residues of PexRD2 to generate variants with differing interaction strengths. These mutants have demonstrated a positive correlation between the ability to interact with MAPKKK $\epsilon$  and the ability to suppress MAPKKK $\epsilon$  signaling-dependent cell death. Furthermore, PexRD2 mutants with reduced ability to bind MAPKKK $\epsilon$  or inhibit its signaling were no longer able to enhance the growth of

*P. infestans* in planta. The PexRD2-like effectors tested were unable to interact with MAPKKK $\epsilon$ . We hypothesize that these and other PexRD2-like effectors, that are predicted to adopt the same overall WY-domain protein fold, may have evolved as kinase interacting modules. Although whether members of the PexRD2 family, other than PexRD2, do indeed target other host kinases remains to be determined. If they do, PexRD2-like effectors may provide useful molecular tools to dissect the role of MAPK signaling in plants. Specificity for different kinases may be encoded in the amino acid residues presented on the surface of the proteins. In support of this, our data showing that PexRD2-like-1a and PexRD2-like-2a do not interact with MAPKKK $\epsilon$  and do not display any of the PexRD2 phenotypes in planta suggest they have a different function.

Detailing the roles of MAPK cascades in plant defense responses is frequently challenging due to genetic redundancy and/or crosstalk associated with plant development (Wang et al., 2007; Qiu et al., 2008; Rodriguez et al., 2010). The best-studied plant MAPKs are *Arabidopsis* MPK3 and MPK6, their orthologs in solanaceous plants, SIPK and WIPK (positive regulators of plant immune pathways), and MPK4 (a negative regulator of plant immune pathways) (Pitzschke et al., 2009; Meng and Zhang, 2013). Double loss-of-function mutations in MPK3 and MPK6 are embryonic lethal, and MPK4 mutants show a severely dwarfed phenotype (Wang et al., 2007; Qiu et al., 2008). Further upstream, double mutation of MAPKKK $\epsilon$ 1 and MAPKKK $\epsilon$ 2 in *Arabidopsis* is pollen-lethal, but plants containing individual mutations to MAPKKK $\epsilon$ 1 or MAPKKK $\epsilon$ 2 show no obvious phenotype (Chaiwongsar et al., 2006). The use of an inducible At-MAPKKK $\epsilon$ 1 construct in the *mapkkk $\epsilon$ 1 mapkkk $\epsilon$ 2* background rescues pollen unviability, but the plants show reduced root length and reduced cell expansion in rosette leaves (Chaiwongsar et al., 2012). Knocking down MAPKKK $\epsilon$  by VIGS in *N. benthamiana* results in a degree of growth inhibition (Melech-Bonfil and Sessa, 2010). Interestingly, we observe that high levels of PexRD2 expression in young leaves can also lead to developmental phenotypes in *N. benthamiana* consistent with retardation of plant growth. Defining whether this is directly linked to PexRD2 interaction with Nb-MAPKKK $\epsilon$ , and whether the effects on growth are linked to or independent of plant immunity, is beyond the scope of this study.

Epistasis analysis has placed MAPKKK $\epsilon$  upstream of MEK2 and SIPK/WIPK in *N. benthamiana* (Melech-Bonfil and Sessa, 2010). Here, we show that overexpression of MAPKKK $\epsilon$  in *N. benthamiana* results in phosphorylation of MAPKs, and this phosphorylation can be suppressed by coexpression with PexRD2. Moreover, whereas PexRD2 suppresses cell death triggered by overexpression of the MAPKKK $\epsilon$  kinase domain, it fails to suppress cell death triggered by MAPKKK $\alpha$  or MEK2<sup>Asp-Asp</sup>. We find that PexRD2 suppresses all readouts of cell death tested that are either triggered by or dependent on MAPKKK $\epsilon$ , while all readouts of cell death tested that are independent of MAPKKK $\epsilon$  are not affected by PexRD2. This suggests a high level of specificity for PexRD2 in interfering with plant immunity-related signaling cascades involving MAPKKK $\epsilon$ .

Our data support the hypothesis that *P. infestans* delivers PexRD2 into host cells to interact with and suppress MAPKKK $\epsilon$  activity, and this is of benefit to the pathogen during infection. In our model for PexRD2 function (Figure 11), this effector interacts with MAPKKK $\epsilon$  to suppress immunity-related signaling by this kinase. We suggest that MAPKKK $\epsilon$  is a target of PexRD2, although

we cannot rule out that MAPKKK $\epsilon$  acts as a helper (Win et al., 2012b) to modify PexRD2 following delivery and this modified protein then perturbs the function of other molecules involved in MAPK cascade signaling.

Both reduction of MAPKKK $\epsilon$  activity (through VIGS) and expression of PexRD2 resulted in enhancing *P. infestans* 88069 growth and suppressing a variety of cell death readouts in *N. benthamiana*. However, we have yet to establish a direct link between MAPKKK $\epsilon$  activity and a specific signaling pathway downstream of oomycete PAMP perception (PRR-mediated immunity) or recognition of an oomycete effector protein (NB-LRR-mediated immunity). Potentially, MAPKKK $\epsilon$  could be important for signaling events following recognition of oomycete PAMPs such as Pep-13 (Halim et al., 2004) and CBEL (Gaulin et al., 2006), as we observed that at least one MAPK is activated by application of *P. infestans* culture filtrate. Alternatively, MAPKKK $\epsilon$  may be required for signaling mediated by one or a subset of the 68 *Solanum* NB-LRRs documented against *P. infestans* (Rodewald and Trognitz, 2013). It is also possible that interfering with MAPKKK $\epsilon$  activity induces a more general perturbation in immunity signaling that is of benefit to the pathogen.

In summary, we identified a *P. infestans* RXLR-WY-type effector, PexRD2, which interacts with MAPKKK $\epsilon$  and perturbs plant immunity associated signaling pathways dependent on this kinase. Either overexpression of PexRD2 or knockdown of MAPKKK $\epsilon$  supports enhanced pathogen growth and suppression of MAPKKK $\epsilon$ -triggered or -dependent cell death readouts in *N. benthamiana*. This study represents a step toward understanding how oomycete RXLR-type effectors directly interact with MAPK cascades, which are well established as key regulators of plant immunity. The next challenge is to better understand the role of PexRD2 and PexRD2-like effectors, and their targets, in the progression of disease in important host crop plants, such as tomato and potato. The ultimate aim of this would be to manipulate these interactions to tip the balance in the coevolutionary arms race between pathogen and host in favor of the plant.

## METHODS

### Bacterial Strains and Growth Conditions

*Escherichia coli*, used for molecular biology, was cultivated in Luria-Bertani medium at 37°C. *Agrobacterium tumefaciens* was grown at 28°C in LB-Lennox broth medium (Lennox, 1955). All binary constructs generated in this study were introduced into *Agrobacterium* strain GV3101 by electroporation.

### Plant Material and Agroinfiltration

*Nicotiana benthamiana* plants were grown in controlled environment rooms at 22°C with 55% humidity and 16 h light or in controlled glasshouses under similar conditions. *Agrobacterium* were incubated in infiltration medium (10 mM magnesium chloride, 10 mM MES, pH 5.6, and 150  $\mu$ M acetosyringone) for at least 1 h prior to infiltration into leaves as described (Van der Hooft et al., 2000).

### *Phytophthora infestans* Infection Assays

*P. infestans* 88069 or *P. infestans* 88069<sup>td</sup> (a stable transformant of *P. infestans* 88069 expressing a tandem-dimer red fluorescent protein) strains were grown on rye Suc agar at 18°C in the dark (Kamoun et al.,

1998). Two leaves of 4- to 5-week old *N. benthamiana* plants were agroinfiltrated at an OD<sub>600</sub> of 0.3 with the binary vector pK7WGF2 (Karimi et al., 2002) (expressing free GFP) on one half of the mid-vein and an effector cloned into pK7WGF2 (expressing N-terminal GFP fusions) into the other half of the same leaf. *Phytophthora* spores were harvested and diluted to 100,000 spores/mL (Kamoun et al., 1998; Schornack et al., 2010). Droplets (10  $\mu$ L) of zoospores were applied onto the abaxial side of detached leaves 24 h postagroinfiltration and incubated for several days on wet paper towels in 100% relative humidity. Lesion areas were determined with GIMP (v2.8) software from white-light photographs. Mycelial growth of *P. infestans* 88069<sup>td</sup> was visualized as described (Chaparro-Garcia et al., 2011). Relative lesion area was calculated by dividing the lesion area at 5 d after zoospore inoculation of leaf tissue transiently expressing the appropriate effector/mutant, by the lesion area achieved on tissue from the same leaf expressing the GFP control at the same time point. Data graphs present the mean lesion area/relative lesion area per infected leaf with error bars representing  $\pm$ se. Either *t* test or one-way ANOVA and Tukey honest significant difference tests were performed to identify statistically significant differences.

### Y2H Screening and Assays

The Proquest two-hybrid system (Invitrogen) was used to detect protein-protein interactions. The original prey library and screening were as described (Bos et al., 2010). PexRD2<sup>21-121</sup> and PexRD2<sup>57-121</sup> were amplified from previously generated plasmid DNA (Boutemy et al., 2011) using primers listed in Supplemental Table 1. PexRD2-like effectors were amplified from *P. infestans* strain T30-4 genomic DNA using primers listed in Supplemental Table 1. The resultant products were cloned into pENTR/D-TOPO and transferred into pDEST 32 using LR clonase. St-MAPKKK $\epsilon$  truncations and Sl-MAPKKK $\alpha$  sequences were amplified using primers listed in Supplemental Table 1 and cloned into pENTR/D-TOPO and transferred to pDEST 22.

### Mutagenesis

Individual point mutants of PexRD2<sup>21-121</sup> and the PexRD2<sup>octa</sup> mutant were either introduced into the wild-type entry clone or synthesized and flanked by the *attB* recombination sites in a pUC57 vector by Genscript. Mutants in the pUC57 background were transferred into pDONR 201 using BP clonase. The PexRD2<sup>hepta</sup> mutant was generated by whole-plasmid mutagenesis using Velocity DNA polymerase (BIOLINE) and pDONR 201: PexRD2<sup>octa</sup> as a template. Methylated parental DNA was removed by *DpnI* treatment. The resultant Glu-90 to Ala mutation was verified by sequencing. Mutant PexRD2 effectors were moved using LR clonase into pDEST 32 for Y2H and pK7WGF2 for in planta assays.

### BiFC

For split-YFP assays, leaves of 4- to 5-week-old *N. benthamiana* plants were infiltrated with *agrobacteria* containing constructs expressing the YN fragment fused to PexRD2, PexRD2-like-1a, or PexRD2-like-2a and the YC fragment fused to the various MAPKKK forms. For each combination, the final OD<sub>600</sub> for each strain was 0.01 for confocal imaging and 0.1 for fluorimeter measurements. Leaf pieces were imaged on a Zeiss 710 microscope 2 d after agroinfiltration using the 514-nm laser line to excite the YFP and a window of 525 to 560 nm to collect emissions. Quantification of fluorescence was performed using a SpectraMax M5 fluorimeter (Molecular Devices). Leaf disks were cut at 2 d post-agroinfiltration and floated abaxial side up on water in 24-well plates. Measurements were made using a well scanning setting taking reads from the top surface. YFP fluorescence was excited at 485 nm and measured at 525 nm. Softmax Pro software (Molecular Devices) was used to collect data that were then exported to Excel for analysis.

### Coimmunoprecipitation of PexRD2

FLAG-epitope tagged PexRD2 in pJL-TRBO (Boutemy et al., 2011) and a GFP-tagged mutant PexRD2 were expressed together in *N. benthamiana* leaves by agroinfiltration. FLAG-epitope tagged proteins were immunoprecipitated by anti-FLAG M2 affinity gel (Sigma-Aldrich) from total protein extracts harvested from leaves 3 d postinoculation (Win et al., 2011). Interacting GFP fusion proteins were detected by immunoblotting of SDS-PAGE separated proteins using anti-GFP antibodies (Invitrogen) as a probe followed by anti-rabbit secondary antibodies conjugated to horseradish peroxidase (Sigma-Aldrich). The expression of effectors in total extract was confirmed using either the procedure above (for GFP-fused effectors) or an anti-FLAG monoclonal antibody conjugated to horseradish peroxidase (Sigma-Aldrich). Chemiluminescent substrate (Thermo Scientific) was added to the blots to visualize positive protein bands after exposure to x-ray films.

### VIGS of *N. benthamiana*

pTRV2:5'-MAPKKK $\epsilon$  used in this study has been described (Melech-Bonfil and Sessa, 2010). A second construct was generated by amplifying a 336-bp fragment of the 3092 to 3427 region of MAPKKK $\epsilon$ 2 from *N. benthamiana* cDNA with the following primers (5'-GGGGgattcCATCA-CAGACTGCGTCAGGT-3' and 5'-GGGGGggttaacTGATTGCATCTGCTC-TCTGG-3'). The resultant PCR product was then ligated into EcoRI and HpaI digested pTRV2, to yield pTRV2:3'-NbMAPKKK $\epsilon$ . VIGS was performed as described previously (Valentine et al., 2004). Briefly, *Agrobacterium* strains harboring pTRV1 vector and pTRV2:GFP, pTRV2:5'-MAPKKK $\epsilon$  or pTRV2:3'-NbMAPKKK $\epsilon$  were mixed in a 1:1 ratio to achieve final OD<sub>600</sub> for each strain of 0.5. The cocultures were then infiltrated into the two largest leaves of 2-week-old plants. The plants were then grown for 2 weeks before using for *P. infestans* infection or cell death assays.

### Cell Death Assays

*Agrobacterium* strains harboring R protein constructs (Cf4, Pto, or R3a) were mixed with those harboring effector protein constructs (Avr4, AvrPto, or AVR3a<sup>KI</sup>, respectively) to achieve final OD<sub>600</sub> values of 1.0 and 0.5, respectively (Gilroy et al., 2011). *Agrobacterium* strains harboring INF1 (Gilroy et al., 2011) or CRN8 (residues 118 to 699) ligated into XmaI- and StuI-digested pEAQ-HT vector (Sainsbury et al., 2009) were diluted to achieve final OD<sub>600</sub> values of 0.5 and 0.3, respectively. *Agrobacterium* mixtures were infiltrated into leaves of VIGS-treated plants, and progression of HR/programmed cell death (PCD) was monitored daily up to 7 d postagroinfiltration. An agroinfiltration site was scored positive for HR/PCD following the development of clear necrosis occupying >50% of the agroinfiltrated area. Data graphs present the mean percentage of total inoculations per plant developing a clear HR with error bars representing  $\pm$ SE of combined data from at least three independent experiments. One-way ANOVA and Tukey honest significant difference tests were performed to identify statistically significant differences.

### Cell Death Suppression Assays

The  $\beta$ -estradiol-inducible S/MAPKKK $\epsilon$ -KD and S/MAPKKK $\epsilon$ -KD<sup>Lys49Arg</sup> constructs used in this study are the same as described (Melech-Bonfil and Sessa, 2010). S/MAPKKK $\epsilon$ -KD<sup>1-332</sup> and S/MAPKKK $\epsilon$ -KD<sup>1-300</sup> were amplified using primers listed in Supplemental Table 1, without a stop codon and ligated into XhoI- and PacI-digested pER8 vector, which already had a double hemagglutinin tag cloned into the PacI and SpeI sites. The S/MAPKKK $\alpha$ -KD and S/MEK2<sup>ASP-ASP</sup> (previously referred to as S/MEK2<sup>DD</sup>) constructs are the same as described those described by del Pozo et al. (2004) and Oh and Martin (2011), respectively.

Cell death activity was confirmed by agroinfiltration of strains harboring the  $\beta$ -estradiol-inducible kinase constructs, and the P19 suppressor of

silencing (Lindbo, 2007), mixed to achieve final OD<sub>600</sub> values of 0.25 and 0.1, respectively. Expression of the kinases was induced by application of 10  $\mu$ M  $\beta$ -estradiol (Sigma-Aldrich) to the leaves at 48 h postagroinfiltration, with additional spray treatments at 48-h intervals when necessary. Progression of cell death was monitored daily up to 7 d after  $\beta$ -estradiol treatment. Effector-mediated suppression of kinase-triggered cell death was assessed in the same way, but with the addition of GFP-PexRD2 (wild type/mutant) or GFP vector control (in pK7WGF2) at a final OD<sub>600</sub> of 0.3, co-agroinfiltrated with the kinase.

*Agrobacterium* strains harboring R protein/effector protein combinations were diluted with *Agrobacterium* harboring the wild type or mutant GFP-PexRD2 or GFP vector control (in pK7WGF2, except AvrPto/Pto HR suppression, which used pB7WGF2) to achieve final OD<sub>600</sub> values of 0.6, 0.3, and 0.3, respectively. *Agrobacterium* strains harboring INF1 or CRN8 were diluted to achieve final OD<sub>600</sub> values, as above, but with the wild type or mutant GFP-PexRD2 or GFP vector control at a 1:1 ratio. Following agroinfiltration of these mixtures into *N. benthamiana* plants, progression of HR/PCD was monitored, scored, and analyzed as described above.

### MAPK Activation Assay

The activation of endogenous MAPKs in *N. benthamiana* following induction of MAPKKK $\epsilon$ -KD expression was assessed using a procedure described (Segonzac et al., 2011). Following agroinfiltration and induction of kinase expression as described above, total protein extracts were separated on a SDS-PAGE gel and transferred to polyvinylidene fluoride membrane. The membrane was probed using anti-pTEP primary antibodies (Cell Signaling), anti-rabbit secondary antibodies conjugated to horseradish peroxidase (Sigma-Aldrich), and a chemiluminescent substrate (Thermo Scientific) in accordance with the manufacturer's instructions.

For PAMP treatment, eight leaf disks of 5 mm in diameter were harvested from 4-week old *N. benthamiana* plants and added to wells of a 96-well microtiter plate, containing 100  $\mu$ L of either MQ-water, 100 nM flg22 peptide, or 100-fold diluted, crude *P. infestans* 88069 culture filtrate (prepared as described in Chaparro-Garcia et al., 2011). These leaf disks were then pooled, and total protein extraction and assessment of the phosphorylation status of MAPKs were conducted as described above.

### Accession Numbers

Sequence data from this article can be found in GenBank/EMBL databases under the following accession numbers: PexRD2 (PITG\_21422, EEEY62542), PexRD2-like-1a (PITG\_14984, EEEY62514), PexRD2-like-2a (PITG\_14787, EEEY62361), potato MAPKKK $\epsilon$  (KJ504180), *S. lycopersicum* MAPKKK $\epsilon$  (ADK36642), *N. benthamiana* MAPKKK $\epsilon$  (ADK36643 and BAM36969), tomato MAPKKK $\alpha$  (AAS78640), and tomato MEK2 (AAU04434).

### Supplemental Data

The following materials are available in the online version of this article.

**Supplemental Figure 1.** PexRD2-Like Bait Proteins Are Expressed and Stable in Yeast.

**Supplemental Figure 2.** PexRD2 and MAPKKK $\epsilon$  Colocalize in the Plant Cell Cytoplasm.

**Supplemental Figure 3.** Localization and Split YFP Fusion Proteins Are Expressed and Stable in Planta.

**Supplemental Figure 4.** Structure-Informed Point Mutants of PexRD2 Can Disrupt the Interaction with MAPKKK $\epsilon$ .

**Supplemental Figure 5.** Mutations within the Structurally Variable Region of the WY-Fold of PexRD2 Reduce the Interaction with MAPKKK $\epsilon$ .

**Supplemental Figure 6.** GFP Fusion Proteins Used for in Planta Assays Are Expressed and Stable.

**Supplemental Figure 7.** Real-Time Quantitative RT-PCR Confirms Specific Silencing of *MAPKKKε*.

**Supplemental Figure 9.** VIGS Experiments to Investigate MAPKKKε-Dependent and MAPKKKε-Independent Cell Death Events.

**Supplemental Figure 10.** PexRD2 Suppresses MAPKKKε-Dependent AvrPto/Pto Hypersensitive Response, but Not MAPKKKε-Independent Cell Death.

**Supplemental Table 1.** Primers Used in This Study.

**Supplemental Methods.**

## ACKNOWLEDGMENTS

We thank the Biotechnology and Biological Science Research Council (BBSRC) (UK; Grants BB/J00453/1, BB/I019557, and BB/G015244), the European Research Council (proposal 294608), the Gatsby Charitable Foundation, the John Innes Foundation, and the Scottish Government Rural and Environment Science and Analytical Services Division for funding in areas relevant to this work. S.R.F.K. is funded by a BBSRC-Doctoral Training Grant (studentship) and the Gatsby Charitable Foundation. We thank Richard Hughes, Angela Chaparro-Garcia, and Liliana Cano for discussion and provision of reagents.

## AUTHOR CONTRIBUTIONS

S.R.F.K., H.M., P.C.B., S.K., P.R.J.B., and M.J.B. designed the research. S.R.F.K., H.M., P.C.B., M.R.A., T.B., O.S., and J.W. performed the research. S.R.F.K., H.M., P.C.B., M.R.A., S.K., P.R.J.B., and M.J.B. analyzed data. S.R.F.K. and M.J.B. wrote the article with contributions/comments from all authors.

Received October 24, 2013; revised January 24, 2014; accepted February 19, 2014; published March 14, 2014.

## REFERENCES

- Armstrong, M.R., et al.** (2005). An ancestral oomycete locus contains late blight avirulence gene *Avr3a*, encoding a protein that is recognized in the host cytoplasm. *Proc. Natl. Acad. Sci. USA* **102**: 7766–7771.
- Asai, T., Tena, G., Plotnikova, J., Willmann, M.R., Chiu, W.L., Gomez-Gomez, L., Boller, T., Ausubel, F.M., and Sheen, J.** (2002). MAP kinase signalling cascade in *Arabidopsis* innate immunity. *Nature* **415**: 977–983.
- Birch, P.R., Rehmany, A.P., Pritchard, L., Kamoun, S., and Beynon, J.L.** (2006). Trafficking arms: Oomycete effectors enter host plant cells. *Trends Microbiol.* **14**: 8–11.
- Boller, T., and Felix, G.** (2009). A renaissance of elicitors: Perception of microbe-associated molecular patterns and danger signals by pattern-recognition receptors. *Annu. Rev. Plant Biol.* **60**: 379–406.
- Bombarely, A., Rosli, H.G., Vrebalov, J., Moffett, P., Mueller, L.A., and Martin, G.B.** (2012). A draft genome sequence of *Nicotiana benthamiana* to enhance molecular plant-microbe biology research. *Mol. Plant Microbe Interact.* **25**: 1523–1530.
- Bos, J.I., et al.** (2010). *Phytophthora infestans* effector AVR3a is essential for virulence and manipulates plant immunity by stabilizing host E3 ligase CMPG1. *Proc. Natl. Acad. Sci. USA* **107**: 9909–9914.
- Boutemy, L.S., King, S.R., Win, J., Hughes, R.K., Clarke, T.A., Blumenschein, T.M., Kamoun, S., and Banfield, M.J.** (2011). Structures of *Phytophthora* RXLR effector proteins: A conserved but adaptable fold underpins functional diversity. *J. Biol. Chem.* **286**: 35834–35842.
- Bozkurt, T.O., Schornack, S., Banfield, M.J., and Kamoun, S.** (2012). Oomycetes, effectors, and all that jazz. *Curr. Opin. Plant Biol.* **15**: 483–492.
- Bozkurt, T.O., Schornack, S., Win, J., Shindo, T., Ilyas, M., Oliva, R., Cano, L.M., Jones, A.M., Huitema, E., van der Hoorn, R.A., and Kamoun, S.** (2011). *Phytophthora infestans* effector AVRblb2 prevents secretion of a plant immune protease at the haustorial interface. *Proc. Natl. Acad. Sci. USA* **108**: 20832–20837.
- Chaiwongsar, S., Otegui, M.S., Jester, P.J., Monson, S.S., and Krysan, P.J.** (2006). The protein kinase genes MAP3K epsilon 1 and MAP3K epsilon 2 are required for pollen viability in *Arabidopsis thaliana*. *Plant J.* **48**: 193–205.
- Chaiwongsar, S., Strohm, A.K., Su, S.H., and Krysan, P.J.** (2012). Genetic analysis of the *Arabidopsis* protein kinases MAP3Kε1 and MAP3Kε2 indicates roles in cell expansion and embryo development. *Front. Plant Sci.* **3**: 228.
- Chang, L., and Karin, M.** (2001). Mammalian MAP kinase signalling cascades. *Nature* **410**: 37–40.
- Chaparro-Garcia, A., Wilkinson, R.C., Gimenez-Ibanez, S., Findlay, K., Coffey, M.D., Zipfel, C., Rathjen, J.P., Kamoun, S., and Schornack, S.** (2011). The receptor-like kinase SERK3/BAK1 is required for basal resistance against the late blight pathogen *Phytophthora infestans* in *Nicotiana benthamiana*. *PLoS ONE* **6**: e16608.
- Cheng, B.P., Yu, X.L., Ma, Z.C., Dong, S.M., Dou, D.L., Wang, Y.C., and Zheng, X.B.** (2012). *Phytophthora sojae* effector Avh331 suppresses the plant defence response by disturbing the MAPK signalling pathway. *Physiol. Mol. Plant Pathol.* **77**: 1–9.
- Cheng, W., Munkvold, K.R., Gao, H., Mathieu, J., Schwizer, S., Wang, S., Yan, Y.B., Wang, J., Martin, G.B., and Chai, J.** (2011). Structural analysis of *Pseudomonas syringae* AvrPtoB bound to host BAK1 reveals two similar kinase-interacting domains in a type III effector. *Cell Host Microbe* **10**: 616–626.
- Chisholm, S.T., Coaker, G., Day, B., and Staskawicz, B.J.** (2006). Host-microbe interactions: Shaping the evolution of the plant immune response. *Cell* **124**: 803–814.
- Cooke, D.E., et al.** (2012). Genome analyses of an aggressive and invasive lineage of the Irish potato famine pathogen. *PLoS Pathog.* **8**: e1002940.
- del Pozo, O., Pedley, K.F., and Martin, G.B.** (2004). MAPKKKα is a positive regulator of cell death associated with both plant immunity and disease. *EMBO J.* **23**: 3072–3082.
- Dodds, P.N., and Rathjen, J.P.** (2010). Plant immunity: Towards an integrated view of plant-pathogen interactions. *Nat. Rev. Genet.* **11**: 539–548.
- Dong, S., et al.** (2011). *Phytophthora sojae* avirulence effector Avr3b is a secreted NADH and ADP-ribose pyrophosphorylase that modulates plant immunity. *PLoS Pathog.* **7**: e1002353.
- Elmore, J.M., and Coaker, G.** (2011). The role of the plasma membrane H<sup>+</sup>-ATPase in plant-microbe interactions. *Mol. Plant* **4**: 416–427.
- Feng, F., Yang, F., Rong, W., Wu, X., Zhang, J., Chen, S., He, C., and Zhou, J.M.** (2012). A Xanthomonas uridine 5'-monophosphate transferase inhibits plant immune kinases. *Nature* **485**: 114–118.
- Frye, C.A., Tang, D., and Innes, R.W.** (2001). Negative regulation of defense responses in plants by a conserved MAPKK kinase. *Proc. Natl. Acad. Sci. USA* **98**: 373–378.
- Gaulin, E., et al.** (2006). Cellulose binding domains of a *Phytophthora* cell wall protein are novel pathogen-associated molecular patterns. *Plant Cell* **18**: 1766–1777.
- Gilroy, E.M., Taylor, R.M., Hein, I., Boevink, P., Sadanandom, A., and Birch, P.R.** (2011). CMPG1-dependent cell death follows

- perception of diverse pathogen elicitors at the host plasma membrane and is suppressed by *Phytophthora infestans* RXLR effector AVR3a. *New Phytol.* **190**: 653–666.
- Gimenez-Ibanez, S., Hann, D.R., Ntoukakis, V., Petutschnig, E., Lipka, V., and Rathjen, J.P.** (2009). AvrPtoB targets the LysM receptor kinase CERK1 to promote bacterial virulence on plants. *Curr. Biol.* **19**: 423–429.
- Göhre, V., Spallek, T., Häweker, H., Mersmann, S., Mentzel, T., Boller, T., de Torres, M., Mansfield, J.W., and Robatzek, S.** (2008). Plant pattern-recognition receptor FLS2 is directed for degradation by the bacterial ubiquitin ligase AvrPtoB. *Curr. Biol.* **18**: 1824–1832.
- Haas, B.J., et al.** (2009). Genome sequence and analysis of the Irish potato famine pathogen *Phytophthora infestans*. *Nature* **461**: 393–398.
- Halim, V.A., Hunger, A., Macioszek, V., Landgraf, P., Nurnberger, T., Scheel, D., and Rosahl, S.** (2004). The oligopeptide elicitor Pep-13 induces salicylic acid-dependent and -independent defense reactions in potato. *Physiol. Mol. Plant Pathol.* **64**: 311–318.
- Hashimoto, M., Komatsu, K., Maejima, K., Okano, Y., Shiraiishi, T., Ishikawa, K., Takinami, Y., Yamaji, Y., and Namba, S.** (2012). Identification of three MAPKKs forming a linear signaling pathway leading to programmed cell death in *Nicotiana benthamiana*. *BMC Plant Biol.* **12**: 103.
- Jin, H., Axtell, M.J., Dahlbeck, D., Ekwenna, O., Zhang, S., Staskawicz, B., and Baker, B.** (2002). NPK1, an MEKK1-like mitogen-activated protein kinase kinase kinase, regulates innate immunity and development in plants. *Dev. Cell* **3**: 291–297.
- Jones, J.D., and Dangl, J.L.** (2006). The plant immune system. *Nature* **444**: 323–329.
- Kamoun, S.** (2006). A catalogue of the effector secretome of plant pathogenic oomycetes. *Annu. Rev. Phytopathol.* **44**: 41–60.
- Kamoun, S., van West, P.Vleeshouwers, V.G., de Groot, K.E., and Govers, F.** (1998). Resistance of *Nicotiana benthamiana* to *Phytophthora infestans* is mediated by the recognition of the elicitor protein INF1. *Plant Cell* **10**: 1413–1426.
- Karimi, M., Inzé, D., and Depicker, A.** (2002). GATEWAY vectors for Agrobacterium-mediated plant transformation. *Trends Plant Sci.* **7**: 193–195.
- Lennox, E.S.** (1955). Transduction of linked genetic characters of the host by bacteriophage P1. *Virology* **1**: 190–206.
- Letunic, I., Doerks, T., and Bork, P.** (2012). SMART 7: Recent updates to the protein domain annotation resource. *Nucleic Acids Res.* **40**: D302–D305.
- Lindbo, J.A.** (2007). TRBO: A high-efficiency tobacco mosaic virus RNA-based overexpression vector. *Plant Physiol.* **145**: 1232–1240.
- Martin, G.B., Bogdanove, A.J., and Sessa, G.** (2003). Understanding the functions of plant disease resistance proteins. *Annu. Rev. Plant Biol.* **54**: 23–61.
- McLellan, H., Boevink, P.C., Armstrong, M.R., Pritchard, L., Gomez, S., Morales, J., Whisson, S.C., Beynon, J.L., and Birch, P.R.** (2013). An RxLR effector from *Phytophthora infestans* prevents re-localisation of two plant NAC transcription factors from the endoplasmic reticulum to the nucleus. *PLoS Pathog.* **9**: e1003670.
- Melech-Bonfil, S., and Sessa, G.** (2010). Tomato MAPKKKε is a positive regulator of cell-death signaling networks associated with plant immunity. *Plant J.* **64**: 379–391.
- Meng, X., and Zhang, S.** (2013). MAPK cascades in plant disease resistance signaling. *Annu. Rev. Phytopathol.* **51**: 245–266.
- Mukhtar, M.S., et al; European Union Effectoromics Consortium** (2011). Independently evolved virulence effectors converge onto hubs in a plant immune system network. *Science* **333**: 596–601.
- Nicaise, V., Roux, M., and Zipfel, C.** (2009). Recent advances in PAMP-triggered immunity against bacteria: Pattern recognition receptors watch over and raise the alarm. *Plant Physiol.* **150**: 1638–1647.
- Oh, C.S., and Martin, G.B.** (2011). Tomato 14-3-3 protein TFT7 interacts with a MAP kinase kinase to regulate immunity-associated programmed cell death mediated by diverse disease resistance proteins. *J. Biol. Chem.* **286**: 14129–14136.
- Oh, S.K., et al.** (2009). In planta expression screens of *Phytophthora infestans* RXLR effectors reveal diverse phenotypes, including activation of the *Solanum bulbocastanum* disease resistance protein Rpi-blb2. *Plant Cell* **21**: 2928–2947.
- Oliva, R., et al.** (2010). Recent developments in effector biology of filamentous plant pathogens. *Cell. Microbiol.* **12**: 705–715.
- Panstruga, R., and Dodds, P.N.** (2009). Terrific protein traffic: The mystery of effector protein delivery by filamentous plant pathogens. *Science* **324**: 748–750.
- Pitzschke, A., Schikora, A., and Hirt, H.** (2009). MAPK cascade signalling networks in plant defence. *Curr. Opin. Plant Biol.* **12**: 421–426.
- Qiu, J.L., Zhou, L., Yun, B.W., Nielsen, H.B., Fill, B.K., Petersen, K., Mackinlay, J., Loake, G.J., Mundy, J., and Morris, P.C.** (2008). Arabidopsis mitogen-activated protein kinase kinases MKK1 and MKK2 have overlapping functions in defense signaling mediated by MEK1, MPK4, and MKS1. *Plant Physiol.* **148**: 212–222.
- Raffaele, S., et al.** (2010). Genome evolution following host jumps in the Irish potato famine pathogen lineage. *Science* **330**: 1540–1543.
- Roche, D.B., Buenavista, M.T., Tetchner, S.J., and McGuffin, L.J.** (2011). The IntFOLD server: An integrated web resource for protein fold recognition, 3D model quality assessment, intrinsic disorder prediction, domain prediction and ligand binding site prediction. *Nucleic Acids Res.* **39**: W171–W176.
- Rodewald, J., and Trognitz, B.** (2013). *Solanum* resistance genes against *Phytophthora infestans* and their corresponding avirulence genes. *Mol. Plant Pathol.* **14**: 740–757.
- Rodriguez, M.C., Petersen, M., and Mundy, J.** (2010). Mitogen-activated protein kinase signaling in plants. *Annu. Rev. Plant Biol.* **61**: 621–649.
- Sainsbury, F., Thuenemann, E.C., and Lomonosoff, G.P.** (2009). pEAQ: Versatile expression vectors for easy and quick transient expression of heterologous proteins in plants. *Plant Biotechnol. J.* **7**: 682–693.
- Saunders, D.G., Breen, S., Win, J., Schornack, S., Hein, I., Bozkurt, T.O., Champouret, N., Vleeshouwers, V.G., Birch, P.R., Gilroy, E.M., and Kamoun, S.** (2012). Host protein BSL1 associates with *Phytophthora infestans* RXLR effector AVR2 and the *Solanum demissum* immune receptor R2 to mediate disease resistance. *Plant Cell* **24**: 3420–3434.
- Schornack, S., van Damme, M., Bozkurt, T.O., Cano, L.M., Smoker, M., Thines, M., Gaulin, E., Kamoun, S., and Huitema, E.** (2010). Ancient class of translocated oomycete effectors targets the host nucleus. *Proc. Natl. Acad. Sci. USA* **107**: 17421–17426.
- Segonzac, C., Feike, D., Gimenez-Ibanez, S., Hann, D.R., Zipfel, C., and Rathjen, J.P.** (2011). Hierarchy and roles of pathogen-associated molecular pattern-induced responses in *Nicotiana benthamiana*. *Plant Physiol.* **156**: 687–699.
- Shan, L., He, P., Li, J., Heese, A., Peck, S.C., Nürnberger, T., Martin, G.B., and Sheen, J.** (2008). Bacterial effectors target the common signaling partner BAK1 to disrupt multiple MAMP receptor-signaling complexes and impede plant immunity. *Cell Host Microbe* **4**: 17–27.
- Thomma, B.P., Nürnberger, T., and Joosten, M.H.** (2011). Of PAMPs and effectors: The blurred PTI-ETI dichotomy. *Plant Cell* **23**: 4–15.
- Valentine, T., Shaw, J., Blok, V.C., Phillips, M.S., Oparka, K.J., and Lacomme, C.** (2004). Efficient virus-induced gene silencing in roots using a modified tobacco rattle virus vector. *Plant Physiol.* **136**: 3999–4009.

- van Damme, M., Bozkurt, T.O., Cakir, C., Schornack, S., Sklenar, J., Jones, A.M., and Kamoun, S. (2012). The Irish potato famine pathogen *Phytophthora infestans* translocates the CRN8 kinase into host plant cells. *PLoS Pathog.* **8**: e1002875.
- van der Hoorn, R.A., and Kamoun, S. (2008). From guard to decoy: A new model for perception of plant pathogen effectors. *Plant Cell* **20**: 2009–2017.
- Van der Hoorn, R.A., Laurent, F., Roth, R., and De Wit, P.J. (2000). Agroinfiltration is a versatile tool that facilitates comparative analyses of Avr9/Cf-9-induced and Avr4/Cf-4-induced necrosis. *Mol. Plant Microbe Interact.* **13**: 439–446.
- Vleeshouwers, V.G., et al. (2008). Effector genomics accelerates discovery and functional profiling of potato disease resistance and *Phytophthora infestans* avirulence genes. *PLoS ONE* **3**: e2875.
- Wang, H., Ngwenyama, N., Liu, Y., Walker, J.C., and Zhang, S. (2007). Stomatal development and patterning are regulated by environmentally responsive mitogen-activated protein kinases in *Arabidopsis*. *Plant Cell* **19**: 63–73.
- Wang, Q., et al. (2011). Transcriptional programming and functional interactions within the *Phytophthora sojae* RXLR effector repertoire. *Plant Cell* **23**: 2064–2086.
- Wang, Y., Li, J., Hou, S., Wang, X., Li, Y., Ren, D., Chen, S., Tang, X., and Zhou, J.M. (2010). A *Pseudomonas syringae* ADP-ribosyltransferase inhibits *Arabidopsis* mitogen-activated protein kinase kinases. *Plant Cell* **22**: 2033–2044.
- Whisson, S.C., et al. (2007). A translocation signal for delivery of oomycete effector proteins into host plant cells. *Nature* **450**: 115–118.
- Win, J., Kamoun, S., and Jones, A.M. (2011). Purification of effector-target protein complexes via transient expression in *Nicotiana benthamiana*. *Methods Mol. Biol.* **712**: 181–194.
- Win, J., Krasileva, K.V., Kamoun, S., Shirasu, K., Staskawicz, B.J., and Banfield, M.J. (2012a). Sequence divergent RXLR effectors share a structural fold conserved across plant pathogenic oomycete species. *PLoS Pathog.* **8**: e1002400.
- Win, J., Chaparro-Garcia, A., Belhaj, K., Saunders, D.G., Yoshida, K., Dong, S., Schornack, S., Zipfel, C., Robatzek, S., Hogenhout, S.A., and Kamoun, S. (2012b). Effector biology of plant-associated organisms: concepts and perspectives. *Cold Spring Harb. Symp. Quant. Biol.* **77**: 235–247.
- Win, J., Morgan, W., Bos, J., Krasileva, K.V., Cano, L.M., Chaparro-Garcia, A., Ammar, R., Staskawicz, B.J., and Kamoun, S. (2007). Adaptive evolution has targeted the C-terminal domain of the RXLR effectors of plant pathogenic oomycetes. *Plant Cell* **19**: 2349–2369.
- Xiang, T., Zong, N., Zou, Y., Wu, Y., Zhang, J., Xing, W., Li, Y., Tang, X., Zhu, L., Chai, J., and Zhou, J.M. (2008). *Pseudomonas syringae* effector AvrPto blocks innate immunity by targeting receptor kinases. *Curr. Biol.* **18**: 74–80.
- Yoshida, K., et al. (2013). The rise and fall of the *Phytophthora infestans* lineage that triggered the Irish potato famine. *Elife* **2**: e00731.
- Zeng, L., Velásquez, A.C., Munkvold, K.R., Zhang, J., and Martin, G.B. (2012). A tomato LysM receptor-like kinase promotes immunity and its kinase activity is inhibited by AvrPtoB. *Plant J.* **69**: 92–103.
- Zhang, J., et al. (2010). Receptor-like cytoplasmic kinases integrate signaling from multiple plant immune receptors and are targeted by a *Pseudomonas syringae* effector. *Cell Host Microbe* **7**: 290–301.
- Zhang, J., et al. (2007). A *Pseudomonas syringae* effector inactivates MAPKs to suppress PAMP-induced immunity in plants. *Cell Host Microbe* **1**: 175–185.
- Zhang, Z., Wu, Y., Gao, M., Zhang, J., Kong, Q., Liu, Y., Ba, H., Zhou, J., and Zhang, Y. (2012). Disruption of PAMP-induced MAP kinase cascade by a *Pseudomonas syringae* effector activates plant immunity mediated by the NB-LRR protein SUMM2. *Cell Host Microbe* **11**: 253–263.
- Zuo, J., Niu, Q.W., and Chua, N.H. (2000). Technical advance: An estrogen receptor-based transactivator XVE mediates highly inducible gene expression in transgenic plants. *Plant J.* **24**: 265–273.

***Phytophthora infestans* RXLR Effector PexRD2 Interacts with Host MAPKKKε to Suppress Plant Immune Signaling**

Stuart R.F. King, Hazel McLellan, Petra C. Boevink, Miles R. Armstrong, Tatyana Bukharova, Octavina Sukarta, Joe Win, Sophien Kamoun, Paul R.J. Birch and Mark J. Banfield  
*Plant Cell* 2014;26;1345-1359; originally published online March 14, 2014;  
DOI 10.1105/tpc.113.120055

This information is current as of September 3, 2014

<b>Supplemental Data</b>	<a href="http://www.plantcell.org/content/suppl/2014/03/10/tpc.113.120055.DC1.html">http://www.plantcell.org/content/suppl/2014/03/10/tpc.113.120055.DC1.html</a>
<b>References</b>	This article cites 80 articles, 30 of which can be accessed free at: <a href="http://www.plantcell.org/content/26/3/1345.full.html#ref-list-1">http://www.plantcell.org/content/26/3/1345.full.html#ref-list-1</a>
<b>Permissions</b>	<a href="https://www.copyright.com/ccc/openurl.do?sid=pd_hw1532298X&amp;issn=1532298X&amp;WT.mc_id=pd_hw1532298X">https://www.copyright.com/ccc/openurl.do?sid=pd_hw1532298X&amp;issn=1532298X&amp;WT.mc_id=pd_hw1532298X</a>
<b>eTOCs</b>	Sign up for eTOCs at: <a href="http://www.plantcell.org/cgi/alerts/ctmain">http://www.plantcell.org/cgi/alerts/ctmain</a>
<b>CiteTrack Alerts</b>	Sign up for CiteTrack Alerts at: <a href="http://www.plantcell.org/cgi/alerts/ctmain">http://www.plantcell.org/cgi/alerts/ctmain</a>
<b>Subscription Information</b>	Subscription Information for <i>The Plant Cell</i> and <i>Plant Physiology</i> is available at: <a href="http://www.aspb.org/publications/subscriptions.cfm">http://www.aspb.org/publications/subscriptions.cfm</a>